



Origin and Li-Enrichment of Selected Oilfield Brines in the Alberta Basin, Canada

AER/AGS Open File Report 2019-01

Origin and Li-Enrichment of Selected Oilfield Brines in the Alberta Basin, Canada

G.F. Huff

Alberta Energy Regulator
Alberta Geological Survey

February 2019

©Her Majesty the Queen in Right of Alberta, 2019
ISBN 978-1-4601-3988-2

The Alberta Energy Regulator / Alberta Geological Survey (AER/AGS), its employees and contractors make no warranty, guarantee or representation, express or implied, or assume any legal liability regarding the correctness, accuracy, completeness or reliability of this publication. Any references to proprietary software and/or any use of proprietary data formats do not constitute endorsement by AER/AGS of any manufacturer's product.

If you use information from this publication in other publications or presentations, please acknowledge the AER/AGS. We recommend the following reference format:

Huff, G.F. (2019): Origin and Li-enrichment of selected oilfield brines in the Alberta Basin, Canada;
Alberta Geological Survey / Alberta Energy Regulator, AER/AGS Open File Report 2019-01, 29 p.

Publications in this series have undergone only limited review and are released essentially as submitted by the author.

Published February 2019 by:

Alberta Energy Regulator
Alberta Geological Survey
4th Floor, Twin Atria Building
4999 – 98th Avenue
Edmonton, AB T6B 2X3
Canada

Tel: 780.638.4491
Fax: 780.422.1459
Email: AGS-Info@aer.ca
Website: www.ags.aer.ca

Contents

1	Introduction.....	1
1.1	Alberta Basin	1
2	Methodology.....	3
2.1	Data Collection and Sources	3
2.2	Hydrologic Regimes	3
3	Oilfield Brines of the Alberta Basin	6
3.1	Central pre-Cretaceous Flow Regime	6
3.1.1	Oilfield Brine Properties	6
3.1.2	Origin of Oilfield Brines.....	6
3.1.3	Li-Enrichment.....	8
3.2	Western pre-Cretaceous Flow Regime	9
3.2.1	Oilfield Brine Properties	9
3.2.2	Origin of Oilfield Brines.....	9
3.2.3	Li-Enrichment.....	9
3.3	Post-Jurassic Flow Regime	10
4	Discussion.....	11
5	Summary	13
6	References.....	14
	Appendix – Plots of Geochemical Data.....	18

Figures

Figure 1.	Location of Western Canada Sedimentary Basin including Alberta and Williston subbasins.	2
Figure 2.	Location of Alberta Basin brine data used in this study.	4
Figure 3.	Location of Li-enriched Alberta Basin brines considered in this report.....	5
Figure 4.	Areal extent of the Devonian Elk Point Basin.....	10
Figure 5.	Conceptual model of brine formation within the Devonian Elk Point Basin.	12
Figure 6.	$\delta^{18}\text{O}$ versus $\delta^2\text{H}$ values showing trends in post-Jurassic and pre-Cretaceous regime brines.....	12
Figure A1-1.	Na/Br versus Cl/Br mass ratios in post-Jurassic and pre-Cretaceous regime brines.....	18
Figure A1-2.	Br versus Cl concentrations in post-Jurassic and pre-Cretaceous regime brines.	18
Figure A1-3.	$\delta^{18}\text{O}$ versus $\delta^2\text{H}$ values in post-Jurassic and pre-Cretaceous regime brines.....	19
Figure A1-4.	Value of $\delta^{18}\text{O}$ versus total dissolved solids concentration in post-Jurassic and pre-Cretaceous regime brines.	19
Figure A1-5.	Concentration of 1/Sr versus $^{87}\text{Sr}/^{86}\text{Sr}$ value in post-Jurassic and pre-Cretaceous regime brines.....	20
Figure A1-6.	Value of $\delta^{18}\text{O}$ versus Cl/Br mass ratio in post-Jurassic and pre-Cretaceous regime brines. .	20
Figure A1-7.	Value of $\delta^{18}\text{O}$ versus K/Br mass ratio in post-Jurassic and pre-Cretaceous regime brines...	21
Figure A1-8.	Value of $\delta^{18}\text{O}$ versus Mg/Br mass ratio in post-Jurassic and pre-Cretaceous regime brines.	21
Figure A1-9.	Value of $\delta^{18}\text{O}$ versus Li/Br mass ratio in post-Jurassic and pre-Cretaceous regime brines. .	22
Figure A1-10.	Total dissolved solids versus Li concentrations in post-Jurassic and pre-Cretaceous regime brines.....	22
Figure A1-11.	Value of $\delta^{18}\text{O}$ versus Li concentration in post-Jurassic and pre-Cretaceous regime brines.	23
Figure A1-12.	Value of specific gravity versus Li concentration in post-Jurassic and pre-Cretaceous regime brines.....	23
Figure A1-13.	Value of $^{87}\text{Sr}/^{86}\text{Sr}$ versus Li concentration in post-Jurassic and pre-Cretaceous regime brines.....	24
Figure A1-14.	Concentrations of Br versus Cl in post-Jurassic and pre-Cretaceous regime brines showing seawater evaporation trajectory.	24

Figure A1-15. Na/Br versus Cl/Br mass ratio showing $\delta^{18}\text{O}$ values in central pre-Cretaceous regime brines.....	25
Figure A1-16. Value of $\delta^{18}\text{O}$ versus specific gravity in post-Jurassic and pre-Cretaceous regime brines.....	25
Figure A1-17. Value of $\delta^{18}\text{O}$ versus $^{87}\text{Sr}/^{86}\text{Sr}$ ratio in post-Jurassic and pre-Cretaceous regime brines.....	26
Figure A1-18. Value of $\delta^2\text{H}$ versus $^{87}\text{Sr}/^{86}\text{Sr}$ ratio in post-Jurassic and pre-Cretaceous regime brines.....	26
Figure A1-19. Value of $^{87}\text{Sr}/^{86}\text{Sr}$ versus K/Br mass ratio in post-Jurassic and pre-Cretaceous regime brines.....	27
Figure A1-20. Value of $^{87}\text{Sr}/^{86}\text{Sr}$ versus Mg/Br mass ratio in post-Jurassic and pre-Cretaceous regime brines.....	27
Figure A1-21. Value of $^{87}\text{Sr}/^{86}\text{Sr}$ versus Li/Br mass ratio in post-Jurassic and pre-Cretaceous regime brines.....	28

Acknowledgements

The author acknowledges the helpful reviews of Brian Smerdon and Tyler Hauck, and the assistance of Jordan Brinsky and Amandeep Singh in figure preparation. Thanks also go to Emily Brock, Stephanie Fleck, Caterina Heikkinen, Gloria Lopez, John Pawlowicz, Jill Weiss and numerous oilfield operators for their facilitation of and assistance in sample collection.

Abstract

Oilfield brines investigated in this study occupy both the pre-Cretaceous and post-Jurassic regional groundwater flow regimes within the Alberta Basin. Samples of pre-Cretaceous groundwater primarily represent Devonian carbonate units while post-Jurassic regime samples primarily represent Cretaceous siliciclastic units. Pre-Cretaceous regime brines located east of the western margin of the Cooking Lake platform (referred to as central-regime brines in this study) show differing properties and have differing evolutionary histories than those lying to the west of the western platform margin (referred to as western-regime brines).

Pre-Cretaceous central-regime brines evolved through progressive evapoconcentration to the point of halite saturation as mid-Devonian seawater moved away from the northwestern open-marine connection of the Devonian Elk Point Basin. Brines nearing the southeastern margin of the Elk Point Basin were enriched in K and Li through dissolution of late-stage evaporite minerals (potash) of the Prairie Evaporite Formation. Following infiltration into the underlying Winnipegosis / Keg River Formation, brines were transported westward by gravitationally-driven flow. Regionally-upward groundwater flow, associated with Laramide tectonism, then forced central-regime brines upward into stratigraphically-higher Devonian carbonates, including the Nisku and Leduc formations.

Pre-Cretaceous western-regime brines evolved through evapoconcentration of mid-Devonian seawater, but not to the point of halite saturation, followed by dissolution of pre-existing halite deposits. K- and Li-enrichment of western-regime brines likely do not represent evaporative processes or interaction with evaporite minerals but, rather, reflect the contribution of hydrothermal fluids.

The composition of post-Jurassic-regime brines can be largely explained as a mixture of underlying pre-Cretaceous regime brines with varying amounts of meteoric water.

1 Introduction

An extensive history of study exists regarding the origins and characteristics of brines within the Alberta Basin of Canada (Figure 1). White (1965) argued that brines of the Alberta Basin are connate in origin while Clayton et al. (1966) argued for complete flushing of the basin. Additional mechanisms advanced to explain the composition of Alberta Basin brines include membrane filtration coupled with halite precipitation (Billings et al., 1969), membrane filtration coupled with freshwater dilution (Hitchon et al., 1971) and diagenetic modification of seawater coupled with freshwater dilution (Hitchon and Friedman, 1969). In more recent work, Connolly et al. (1990a; 1990b) proposed evaporation of seawater beyond halite saturation with subsequent dilution by meteoric water. Michael and Bachu (2002) proposed evapoconcentration of seawater combined with the effects of dolomitization, halite dissolution and dilution with meteoric water. Michael et al. (2003) proposed seawater evapoconcentration beyond gypsum but less than halite saturation combined with the effects of dolomitization, clay mineral and gypsum dewatering, sulphate reduction and halite dissolution. Gupta et al. (2012) proposed the presence of brine endmembers formed through evapoconcentration of seawater beyond halite saturation and through dissolution of halite coupled with mixing with seawater and meteoric water. The numerous and varied mechanisms proposed for the origin of Alberta Basin brines reflect the potentially complex history of these waters.

Enrichment of oilfield brines in Li has been documented in the Devonian of the Williston Basin in North Dakota, the Jurassic Smackover Formation of the US Gulf Coast, the Cretaceous of Texas and the southern coastal plain of Israel (Collins, 1976; Chan et al., 2002; Garrett, 2004). Li-enrichment of brines within Devonian carbonates of the Alberta Basin has been reported by Hitchon et al. (1993), Underschultz et al. (1994), Bachu (1995), Eccles and Berhane (2011) and Huff (2016). Hitchon et al. (1993) observed that Li concentrations increased with increasing brine salinity. Eccles and Berhane (2011) observed that Li concentrations in brines in the Swan Hills Formation correlated with radiogenically-enriched $^{87}\text{Sr}/^{86}\text{Sr}$ values and noted that these brines were associated with dolomitized carbonates. Furthermore, Eccles and Berhane (2011) argued that these Li-enriched brines had not been evapoconcentrated past halite saturation, lacked a meteoric water component and had become Li-enriched through mixing with fluids expelled from crystalline basement rocks. Huff (2016) proposed dissolution of late-stage evaporate minerals into evapoconcentrated seawater, followed by various degrees of dilution with meteoric water, in the formation of brines in the Leduc and Nisku Formations containing >50 mg/kg Li.

Increasing demand for Li has created an interest in the possible commercial exploitation of Li-enriched oilfield brines. This study uses published data to further investigate potential mechanisms for the generation of Li-enriched brines of the Alberta Basin. Brine samples used in this study were acquired from the Devonian Wabamun Group and Swan Hills, Nisku and Leduc formations; and the Cretaceous Mannville Group, and Viking and Cardium formations.

1.1 Alberta Basin

The Alberta Basin is bordered to the west by the Rocky Mountain Fold and Thrust Belt, to the northeast by Precambrian basement rocks and to the southeast by the Sweetgrass / Bow Island Arch. The Alberta Basin forms the western part of the Western Canada Sedimentary Basin (WCSB), which also contains the Williston Basin to the east (Figure 1). The Alberta Basin consists of a wedge of westward-thickening and westward-dipping Paleozoic through Cenozoic sediments (Wright et al., 1994). An extensive unconformity separates pre-Cretaceous from post-Jurassic deposits throughout most of the WCSB (Poulton et al., 1994). The pre-Cretaceous deposits consist primarily of carbonates, evaporates and shales while the post-Jurassic deposits range from coarse- to fine-grained siliciclastics. Jurassic through Eocene tectonic events (Price, 1994; Pană and van der Pluijm, 2015) have imparted a westerly dip to units above and below the basin-wide unconformity. Devonian units within the Alberta Basin include a series of well-developed dolomitized and undolomitized reef structures many of which rest on extensive platform carbonate deposits.

Bachu (1995; 1999) recognized distinct pre-Cretaceous and post-Jurassic mesoscale hydrologic regimes within the Alberta Basin. Fluid flow in the pre-Cretaceous regime takes place largely through Carboniferous and Devonian carbonates and is thought to be driven by a combination of topographic relief, tectonic compression and density gradients. Fluid flow in the post-Jurassic regime takes place largely through Cretaceous to Tertiary clastics and is thought to be principally driven by modern-day topographic relief. Hitchon (1969; 1984) proposed deep incursion of meteoric water into the subsurface of the southwestern Alberta Basin driven by topographic changes associated with Laramide tectonics. Evidence exists for the presence of a post-Laramide, and possibly modern-day flow system, from Devonian carbonates upward across the basin-wide unconformity into overlying Cretaceous siliciclastics (Bachu 1995; 1999; Rostron and Tóth, 1996; 1997). Density-driven downdip flow of brines in Devonian carbonates of the Alberta Basin has been suggested by Michael et al. (2003). Simulations of subsurface fluid flow indicate a Devonian age of formation for brines hosted in the Devonian carbonates of the southwestern Alberta Basin (Gupta et al., 2012).



Figure 1. Location of Western Canada Sedimentary Basin including Alberta and Williston subbasins.

2 Methodology

2.1 Data Collection and Sources

Data used in this study include analyses of oilfield brine samples from Alberta Basin formations of the Devonian (Wabamun Group and Swan Hills, Nisku, Slave Point and Leduc formations) and Cretaceous (Mannville Group and Viking and Cardium formations) periods, collected by the Alberta Geological Survey (AGS) between 2011 and 2016 (Huff et al., 2011; 2012; 2019). Additional data used in this study include analyses of brines from the Swan Hills Formation of Alberta (Eccles and Berhane, 2011).

Analyses reported by Huff et al. (2011; 2012; 2019) were obtained from brine samples collected from mature oil wells that had been in production for a minimum of six months since any major treatment or chemical stimulation. All additives to the wellbore or well stream were discontinued for a minimum of 24 hours prior to sampling. Brine samples were collected and preserved using a slightly modified version of the method described by Lico et al. (1982). The results of all analyses reported by Huff et al. (2011; 2012; 2019) have charge balance errors of no more than 5 %. Further analytical details are described in Huff et al. (2011; 2012; 2019). Specific gravities of Swan Hills brines were estimated from salinity data reported by Eccles and Berhane (2011) using specific gravities of aqueous NaCl solutions at 20°C (Weast and Astle, 1978, p. D299-D300). The locations of brine samples collected within Alberta and used in this study are shown in [Figure 2](#).

2.2 Hydrologic Regimes

The results of this study are organized by hydrologic regime with subdivision of the pre-Cretaceous regime into central and western parts, as differentiated by the western margin of the Cooking Lake carbonate platform ([Figure 2](#)). Brine samples from the central pre-Cretaceous flow regime used in this study dominantly represent the Devonian Cooking Lake, Leduc and Nisku formations. Brine samples from the western pre-Cretaceous flow regime used in this study represent the Devonian Leduc, Nisku, Slave Point, and Swan Hills formations, and the Wabamun Group. Brine samples from the post-Jurassic flow regime used in this study represent the Viking and Cardium formations and the Mannville Group.

Brines containing >50 mg/L Li are considered as Li-enriched for the purpose of this study. In this study Li enrichment was observed solely in oilfield brines of the pre-Cretaceous flow regime. The location of Li-enriched (≥ 50 mg/L Li) brines considered in this report are shown in [Figure 3](#). Geochemical evolution of Li-enriched brines will be discussed within the context of available information on the compositions of brines, regimes of groundwater flow and potentially-related evaporite deposits.

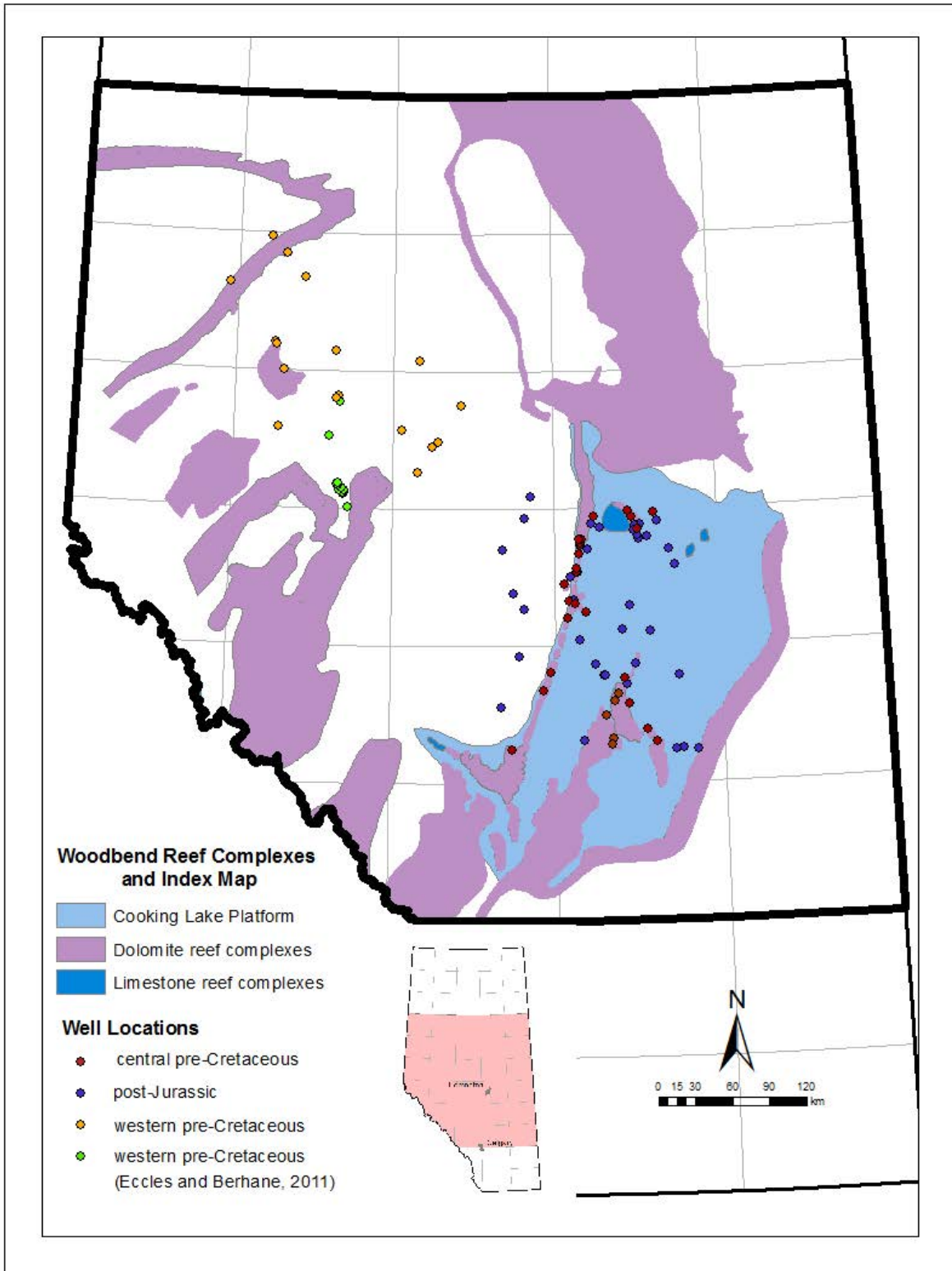


Figure 2. Location of Alberta Basin brine data used in this study, colour coded to hydrologic regime. Extent of Woodbend reef complexes taken from Switzer et al. (1994).

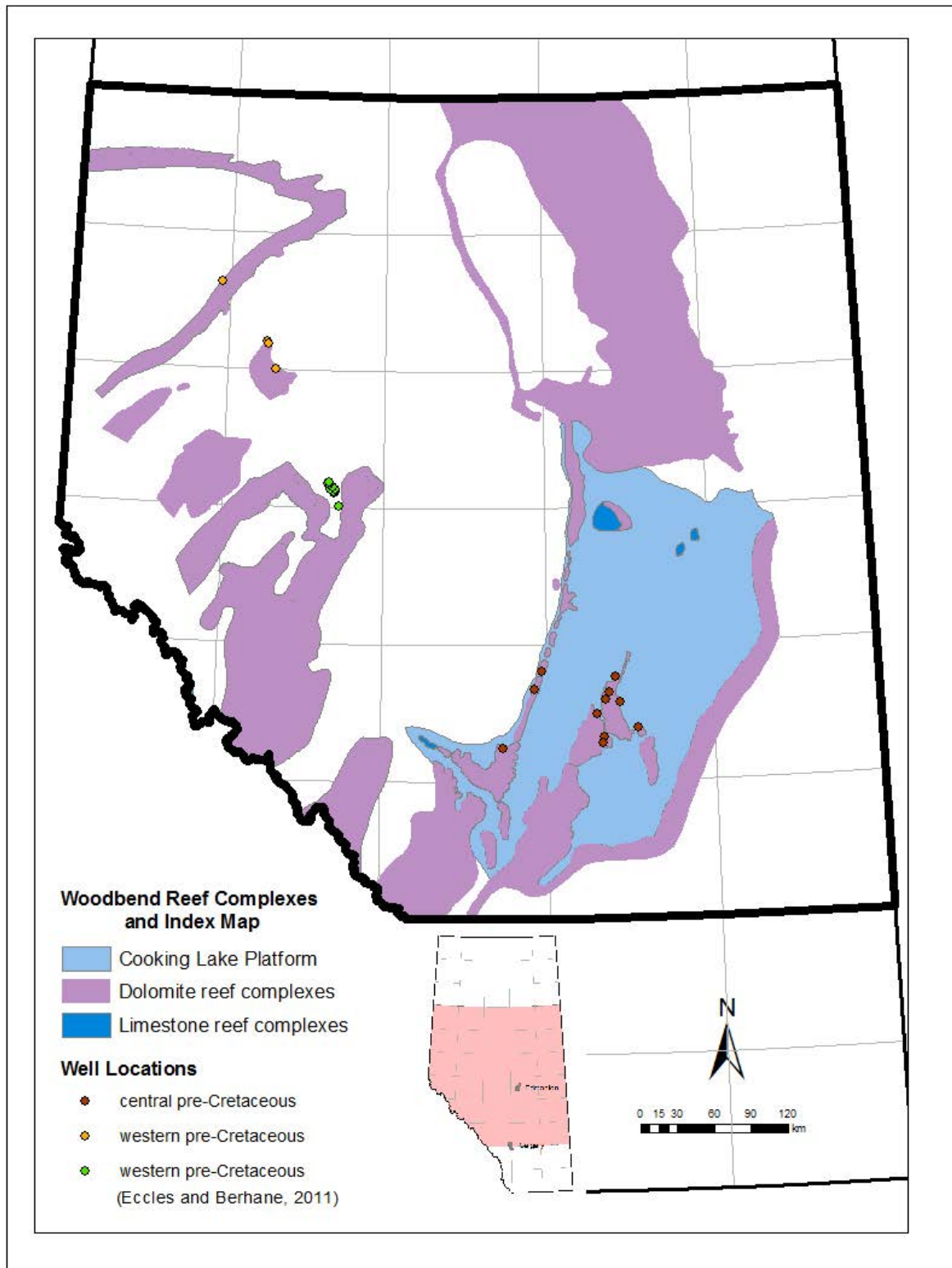


Figure 3. Location of Li-enriched Alberta Basin brine data considered in this report. Extent of Woodbend reef complexes taken from Switzer et al. (1994).

3 Oilfield Brines of the Alberta Basin

The oilfield brine data are presented and discussed in this section. The discussion is organized by central and western pre-Cretaceous flow regime and post-Jurassic flow regime. Each sub-section summarizes the geochemical data and discusses the origin of brines and Li-enrichment. Bivariate plots of the geochemical systematics are presented in the Appendix.

3.1 Central pre-Cretaceous Flow Regime

3.1.1 Oilfield Brine Properties

Brines of the central pre-Cretaceous flow regime examined in this study dominantly plot below and to the left of modern seawater in the Na-Cl-Br system (Figure A1-1). Central-regime brines with Cl concentrations greater than approximately 100 000 mg/L show a pattern of relative Br enrichment (Figure A1-2). Central-regime brines plot to the right of the global meteoric water line (Craig, 1961) and generally converge toward the meteoric water line with decreasing $\delta^{18}\text{O}$ values (Figure A1-3).

Concentrations of total dissolved solids are generally less than 175 000 mg/L in central-regime brines having $\delta^{18}\text{O}$ values $<0\text{‰}$, and greater than 175 000 mg/L in central-regime brines having $\delta^{18}\text{O}$ values $>0\text{‰}$ (Figure A1-4). Values of $^{87}\text{Sr}/^{86}\text{Sr}$ vary little in central-regime brines (Figure A1-5) and occur within a range consistent with mid-Devonian seawater as reported by Burke et al. (1982).

For central-regime brines showing $\delta^{18}\text{O}$ values $>0\text{‰}$, Cl/Br mass ratios range from approximately 100 to 150 (Figure A1-6), mass ratios of K/Br range from approximately 2 to 8 (Figure A1-7), mass ratios of Mg/Br range from approximately 3 to 4 (Figure A1-8), and mass ratios of Li/Br range from approximately 0.025 to 0.10 (Figure A1-9). K/Br, Mg/Br and Li/Br mass ratios generally increase with increasing $\delta^{18}\text{O}$ values in central-regime brines having $\delta^{18}\text{O}$ values $>0\text{‰}$.

Central-regime brines containing $>50\text{ mg/L}$ Li are associated with TDS concentrations $>175\text{ 000 mg/L}$ (Figure A1-10), $\delta^{18}\text{O}$ values $>0\text{‰}$ (Figure A1-11) and specific gravities >1.125 (Figure A1-12). There is no systematic relationship between Li concentrations and $^{87}\text{Sr}/^{86}\text{Sr}$ values in central-regime brines (Figure A1-13).

3.1.2 Origin of Oilfield Brines

Plotting positions below and to the left of modern seawater in the Na-Cl-Br system are typically interpreted to represent samples that have acquired salinity through evapoconcentration of seawater beyond halite saturation (Walter, 1990). The pattern of Br and Cl concentrations, as superimposed on the evaporation trajectory of modern seawater (McCaffrey et al., 1987), is also consistent with evapoconcentration of seawater beyond halite saturation followed by dilution with meteoric water (Figure A1-14). Gupta et al. (2012) drew similar conclusions based on Br-Cl systematics of brines in the Alberta Basin. However, Gupta et al. (2012) pointed out the potential non-uniqueness of this approach owing to possible subsequent dissolution of subsurface evaporites. Assuming no substantial influence from the dissolution of subsurface evaporites, data shown in Figures A1-2 and A1-14 suggests central-regime brines may have originated from seawater evapoconcentrated by 11 to 35 times. This degree of evapoconcentration represents conditions of saturation with respect to halite, but does not reach saturation with respect to potash minerals (Holser, 1979a). The relationships between $\delta^{18}\text{O}$ values and $\delta^2\text{H}$ values (Figure A1-3) and between $\delta^{18}\text{O}$ values and total dissolved solids (Figure A1-4) suggests that the compositions of central-regime brines having $\delta^{18}\text{O}$ values $<0\text{‰}$ have been influenced by mixing with meteoric water.

Superposition of $\delta^{18}\text{O}$ values onto a plot of the Na-Cl-Br systematics of central-regime brines shows a general, but not definite, trend toward more positive $\delta^{18}\text{O}$ values with increasing apparent effects of evapoconcentration (Figure A1-15). Generally decreasing $\delta^{18}\text{O}$ values of brines having Cl/Br ratios less than 130 could be explained by the reversal of $\delta^{18}\text{O}$ values known to happen under extreme evaporative

conditions (Hosler, 1979b) or by mixing with meteoric water. Many samples having Cl/Br ratios greater than 175 in Figure A1-6 have $\delta^{18}\text{O}$ values <0 ‰, possibly reflecting the effects of mixing with meteoric water. However, the observed clustering of samples having $\delta^{18}\text{O}$ values <0 ‰ (Figure A1-15) requires a more systematic explanation. Though somewhat controversial, evidence exists that the $\delta^{18}\text{O}$ value of Devonian seawater may have been more negative than that of modern seawater (Lecuyer and Allemand, 1999; Wallmann, 2001; Selleck and Koff, 2008). An initial $\delta^{18}\text{O}$ value more negative than that of modern seawater may have allowed substantially-evapoconcentrated mid-Devonian seawater to retain $\delta^{18}\text{O}$ values <0 ‰.

K/Br (Figure A1-7) and Mg/Br (Figure A1-8) mass ratios of central-regime brines systematically increase as $\delta^{18}\text{O}$ increases from 0 ‰ to more positive values. Data of McCaffrey et al. (1987) show that K/Br and Mg/Br mass ratios remain fundamentally unaltered during evapoconcentration-driven precipitation of halite from modern seawater and then begin to decline once further evaporation brings about the onset of potash mineral formation. The behavior of modern seawater suggests that the changes observed in K/Br and Mg/Br mass ratios of central-regime brines having $\delta^{18}\text{O}$ values >0 ‰ cannot be explained solely by progressive evapoconcentration of a relatively homogenous initial solution resembling modern seawater.

The mid-Devonian Prairie Evaporite Formation is an extensive evaporite succession that includes marine salt deposited over carbonates of the Winnipegosis / Keg River Formation within the Devonian Elk Point Basin (Figure 3), which covers parts of Alberta, Saskatchewan, and a small portion of the northern USA (Holter, 1969; Hamilton, 1971; Grobe, 2000). The approximate northern margin of the Elk Point Basin, as defined by the zero edge of Elk Point Formation rocks, is shown in Figure 4. The Prairie Evaporite Formation consists of halite, sylvite, carnallite, anhydrite, dolomite and clay minerals (Holter, 1969). The source of open-marine waters in the Elk Point Basin was likely to the north and northwest in mid-Devonian time (Maiklem, 1971). Potash mineralization within the Prairie Evaporite Formation is confined to the (modern-day) southeastern part of the Elk Point Basin reflecting the effect of progressive evaporation of seawater as it moved away from the northwestern area of open-marine connection (Holter, 1969). Numerous authors have cited evidence for post-depositional remobilization or dissolution of late-stage evaporite minerals within the Prairie Evaporite (Van der Plank, 1962; Schwerdtner, 1964; Streeton, 1967; Wardlaw, 1968; Hamilton, 1971).

Central-regime brines apparently arise from the interaction of evapoconcentrated mid-Devonian seawater and evaporite minerals with the possible input of various amounts of meteoric water. Marine water entering the Elk Point Basin would have been subject to increasing degrees of evapoconcentration while moving southeastward away from the area of open-marine connection. Upon reaching halite saturation, continued evapoconcentration would have progressively decreased Cl/Br and Na/Br mass ratios and initially shifted $\delta^{18}\text{O}$ toward more positive values. Further evapoconcentration would, at some point, begin to shift $\delta^{18}\text{O}$ toward more negative values. Under this scenario, only relatively more evapoconcentrated seawater would typically have reached the current known area of potash mineralization within the Prairie Evaporite Formation. Dissolution of potash minerals into relatively more evapoconcentrated mid-Devonian seawater could explain the observed elevation in K/Br and Mg/Br mass ratios in central-regime brines having $\delta^{18}\text{O}$ values >0 ‰. It is worth noting that Mg/Br mass ratios observed in central-regime brines are well below values expected on evapoconcentration of modern seawater to halite saturation. Extensive dolomitization present in the Devonian carbonates of the WCSB may account for the apparent Mg depletion of central-regime brines.

The observed range of Cl/Br and Na/Br mass ratios and $\delta^{18}\text{O}$ values in central-regime brines requires infiltration of mid-Devonian seawater evapoconcentrated to varying degrees into the underlying Winnipegosis / Keg River carbonates. Brines introduced into the Winnipegosis / Keg River carbonates may have initially had specific gravities >1.12 prior to substantial dilution with meteoric water (Figure A1-16). Tectonism beginning in Jurassic time imparted a westward dip to pre-Cretaceous geologic units including the Winnipegosis / Keg River Formation, potentially allowing dense evaporative brines to migrate westward. Density-driven downdip flow of brines in Devonian carbonates of the Alberta Basin

has also been suggested by Michael et al. (2003). Hitchon (1969; 1984) proposed deep incursion of meteoric water into the subsurface of the southwestern Alberta Basin driven by topographic changes associated with Laramide tectonics. Evidence exists for the presence of a post-Laramide, and possibly modern-day, flow system from Devonian carbonates upward into overlying Cretaceous siliciclastics (Bachu 1995; 1999; Rostron and Tóth, 1996). Gravity-driven westward flow beginning in Jurassic time, followed by the incursion and upward cross-formational flow of meteoric water through Devonian carbonates beginning in Cretaceous time, could account for the observed dilution and emplacement of evaporative brines in the permeable reef structures of the Leduc and Nisku Formations.

3.1.3 Li-Enrichment

Concentrations of Li in central-regime brines show no apparent correlation with $^{87}\text{Sr}/^{86}\text{Sr}$ values (Figure A1-13) suggesting that Li is not derived from interaction with silicate minerals. Data presented by McCaffrey et al. (1987) show that evapoconcentrating modern seawater well into the range of potash-mineral saturation produces <20 mg/L Li in the resulting residual brine. The pattern of change in Li/Br mass ratios of central-regime brines with increasing apparent evapoconcentration (Figure A1-9) is markedly similar to those observed for K/Br and Mg/Br mass ratios (Figures A1-7 and A1-8). These observed similarities in patterns of change in selected mass ratios, combined with the presence of Li concentrations that can reach >50 mg/L, suggest that Li enrichment of central-regime brines did not occur through a simple evapoconcentrative process.

Data from Horita et al. (1996) show Li/Br mass ratios of 0.10 to 0.15 in fluid inclusions from apparently diagenetically-altered halite within the Prairie Evaporite Formation. In contrast, the Li/Br mass ratio of modern seawater is approximately 0.003 (Drever, 1982, p. 234). Fluid inclusion compositions reported by Horita et al. (1996) infer the action of a process that has increased aqueous Li concentrations with respect to Br relative to those found in modern seawater. Li/Br mass ratios approach values of 0.10 in central-regime brines showing the greatest $\delta^{18}\text{O}$ values (Figure A1-9). Mass ratios of K/Br in fluid inclusions range from approximately 1 to 4 (Horita et al., 1996) falling within the low end of the range of K/Br mass ratios of central-regime brines having $\delta^{18}\text{O}$ values >0 ‰ (Figure A1-7). Mass ratios of Mg/Br in fluid inclusions range from approximately 50 to 60 (Horita et al., 1996) greatly exceeding the range of Mg/Br mass ratios of central-regime brines having $\delta^{18}\text{O}$ values >0 ‰ (Figure A1-8). As previously discussed herein, the extensive dolomitization of Devonian carbonates within the WCSB could serve as a substantial sink for Mg.

As has been argued for central-regime brines, simple evapoconcentration would not produce elevated Li/Br, K/Br or Mg/Br mass ratios observed in fluid inclusions within diagenetically-altered halite of the Prairie Evaporite Formation. Li tends to be highly soluble even in brines that have been evapoconcentrated to potash-minerals saturation (Hosler, 1979b, p. 321). However, evidence also exists for the significant partitioning of Li into late-stage evaporite minerals (Vengosh et al., 1992). Additionally, Yu et al. (2015) have experimentally shown that a variety of Li-enriched salts, including a Li analog of carnallite, can form under conditions simulating extreme evaporation. It is reasonable to conclude that Li would be partitioned into, and concentrated in, the most soluble evaporite mineral phases forming as an evapoconcentrating brine approaches dryness. It is also reasonable to assume that such late-phase Li-enriched phases would be highly soluble into seawater evaporated to, but not beyond, halite saturation. Available information suggests that central-regime brines became Li-enriched through dissolution of Li-bearing late-stage evaporite minerals into mid-Devonian seawater evapoconcentrated to, but not beyond, halite saturation. Preservation of Li concentrations >50 mg/L in modern-day central-regime brines appears to be strongly influenced by the degree of mixing of brines with meteoric water.

3.2 Western pre-Cretaceous Flow Regime

3.2.1 Oilfield Brine Properties

Brines of the western pre-Cretaceous flow regime examined in this study dominantly plot above and to the right of modern seawater in the Na-Cl-Br system (Figure A1-1). No apparent trend is present in Cl/Br mass ratios with increasing $\delta^{18}\text{O}$ values in western-regime brines (Figure A1-4). Western-regime brines plot slightly above the Cl-Br evaporation trajectory of modern seawater (McCaffrey et al., 1987) (Figure A1-14).

Values of $^{87}\text{Sr}/^{86}\text{Sr}$ show little variation with $\delta^{18}\text{O}$ values, and fall within the range of values consistent with mid-Devonian seawater (Burke et al., 1982), in western-regime brines having $\delta^{18}\text{O}$ values $<-2\text{‰}$ (Figure A1-17). In contrast, increasing $^{87}\text{Sr}/^{86}\text{Sr}$ values substantially correspond with increasing $\delta^{18}\text{O}$ values in western-regime brines having $\delta^{18}\text{O}$ values $>-2\text{‰}$ (Figure A1-17). Values of $^{87}\text{Sr}/^{86}\text{Sr}$ show little variation with $\delta^2\text{H}$ values, and fall within the range of values consistent with mid-Devonian seawater (Burke et al., 1982), in western-regime brines having $\delta^2\text{H}$ values $<-50\text{‰}$ (Figure A1-18). Values of $^{87}\text{Sr}/^{86}\text{Sr}$ more radiogenic than mid-Devonian seawater occur in association with $\delta^2\text{H}$ values $>-50\text{‰}$ (Figure A1-18). Values of $\delta^2\text{H}$ show no systematic change with increasing relative amounts of ^{87}Sr in western-regime brines having $^{87}\text{Sr}/^{86}\text{Sr}$ values more radiogenic than mid-Devonian seawater (Figure A1-18). Mass ratios of K/Br (Figure A1-19) and Li/Br (Figure A1-21) substantially correspond with increasing $^{87}\text{Sr}/^{86}\text{Sr}$ values in western-regime brines having $^{87}\text{Sr}/^{86}\text{Sr}$ values more radiogenic than mid-Devonian seawater. Mass ratios of Mg/Br show no systematic variation with increasing $^{87}\text{Sr}/^{86}\text{Sr}$ values in western-regime brines having $^{87}\text{Sr}/^{86}\text{Sr}$ values more radiogenic than mid-Devonian seawater (Figure A1-20).

3.2.2 Origin of Oilfield Brines

Plotting positions above and to the right of modern seawater in the Na-Cl-Br system are typically interpreted to represent samples that have acquired salinity through dissolution of halite (Walter, 1990). Observed Cl and Br variations, coupled with the presence of $^{87}\text{Sr}/^{86}\text{Sr}$ values characteristic of mid-Devonian seawater where $\delta^{18}\text{O}$ values are $<-2\text{‰}$, suggest that western-regime brines formed through dissolution of halite into mid-Devonian seawater. The presence of $\delta^{18}\text{O}$ values $<-2\text{‰}$ may be reflective of some degree of evaporation or may be reflective of mid-Devonian seawater values being initially $<0\text{‰}$. Abundant halite exists within the Devonian of the WCSB (Hamilton, 1971; Grobe, 2000) (Figure 4) with which potentially-evapoconcentrated mid-Devonian seawater could have interacted. Similar to central-regime brines, western-regime brines having $\delta^{18}\text{O}$ values $<-2\text{‰}$ appear to have been substantially effected by mixing with meteoric water (Figure A1-3).

Observed increases in K/Br and Li/Br mass ratios and $\delta^{18}\text{O}$ values with increasingly radiogenic $^{87}\text{Sr}/^{86}\text{Sr}$ values, coupled with relatively constant $\delta^2\text{H}$ values, suggest the influence of a hydrothermal fluid(s) on the composition of western-regime brines. The contribution of hydrothermal fluids to the evolution of brines in the Swan Hills Formation has been previously suggested by Eccles and Berhane (2011). In addition, Machel et al. (1996; 2001) cite evidence for the involvement of hydrothermal fluids in the diagenesis of Devonian carbonates near the western margin of the WCSB.

3.2.3 Li-Enrichment

Increasing mass ratios of Li/Br (Figure A1-21) and Li concentrations (Figure A1-13) with increasingly radiogenic $^{87}\text{Sr}/^{86}\text{Sr}$ values strongly suggests that Li-enrichment in western-regime brines is associated with the presence and amount of hydrothermal fluids present. Eccles and Berhane (2011) reached a similar conclusion regarding the origin of Li-enrichment in brines of the Swan Hills Formation.

3.3 Post-Jurassic Flow Regime

Post-Jurassic flow regime brines generally have dissolved solids concentrations $<175\,000$ mg/L (Figure A1-4) and specific gravities <1.1 (Figure A1-16). Post-Jurassic regime brines plot below and to the left of modern seawater in the Na-Cl-Br system (Figure A1-1). Post-Jurassic flow regime brines consistently show $\delta^{18}\text{O}$ values <0 ‰ and systematically converge toward the global meteoric water line as $\delta^{18}\text{O}$ values decrease (Figure A1-3). Post-Jurassic regime brines show $^{87}\text{Sr}/^{86}\text{Sr}$ values consistent with those expected in mid-Devonian seawater (Figure A1-5).

The overall composition of post-Jurassic flow regime brines is best explained as a mixture of underlying pre-Cretaceous-regime brines with varying amounts of meteoric water. Connolly et al (1990a; 1990b) reached similar conclusions regarding the origin of selected brines from the Cretaceous formations of the WCSB. Upward movement of pre-Cretaceous-regime brines along with concurrent mixing with meteoric water is consistent with the deep meteoric water incursion proposed by Hitchon (1969; 1984) and the proposed presence of upward flow from Devonian into overlying Cretaceous units (Bachu 1995; 1999; Rostron and Tóth, 1996; 1997).

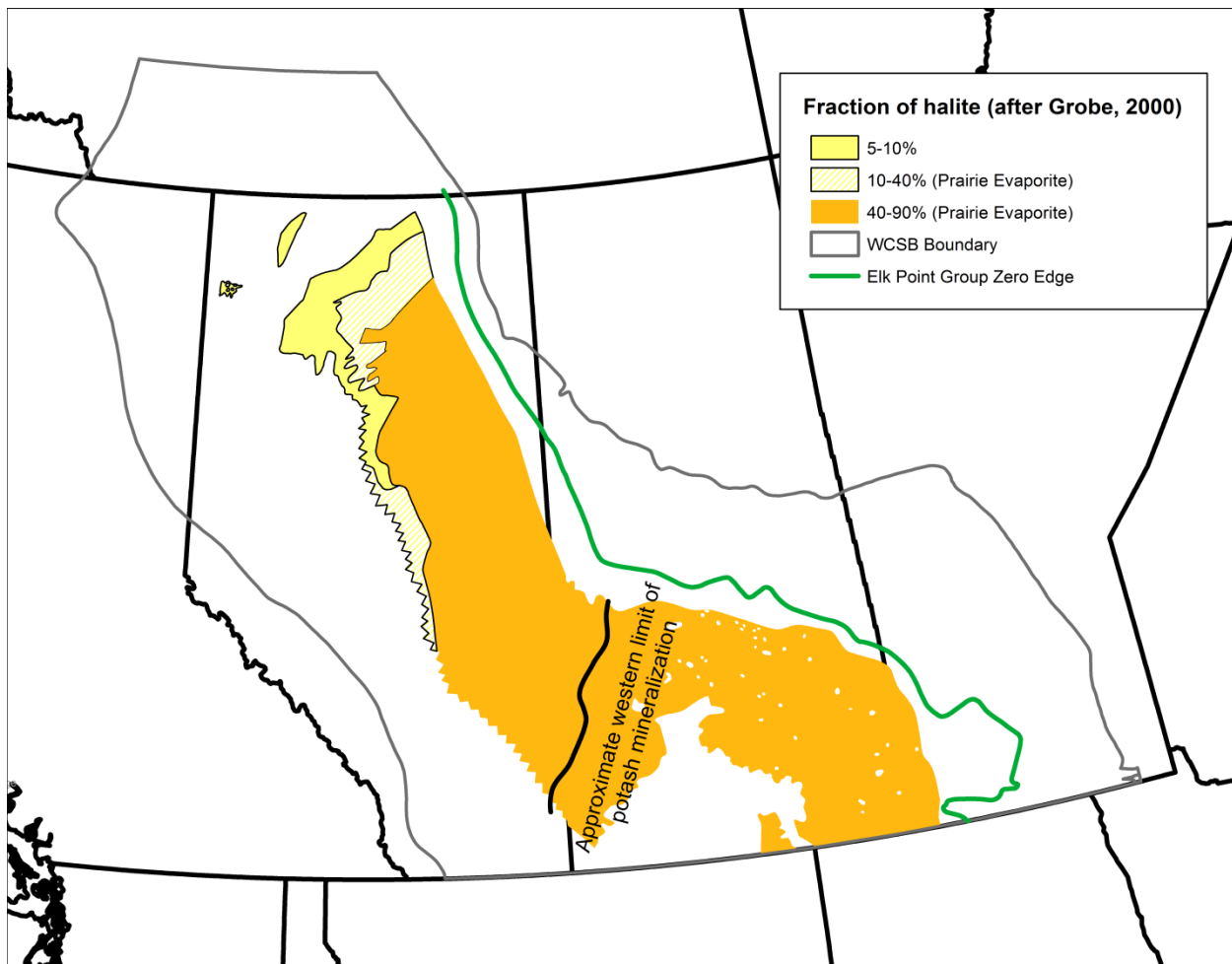


Figure 4. Areal extent of the Devonian Elk Point Basin showing extent of halite and potash mineralization (after Grobe, 2000).

4 Discussion

The composition of brines preserved within selected Devonian carbonates of the WCSB could be viewed as reflective of the evolution of mid-Devonian seawater as it moved across the Devonian Elk Point Basin ([Figure 5](#)). Brines present in the western pre-Cretaceous regime may reflect mid-Devonian seawater derived from relatively near the open-marine connection of the Elk Point Basin. Seawater derived from relatively near the open-marine portion of the basin margin would have undergone relatively little evapoconcentration, potentially allowing for subsequent modification through dissolution of halite. Brines present in the central pre-Cretaceous regime may reflect mid-Devonian seawater subjected to progressively greater degrees of evaporation as it traversed along the Elk Point Basin. Brines derived from seawater traversing the Elk Point Basin show evidence of evapoconcentration to, but not exceeding, halite saturation. Brines having elevated K/Br and Li/Br mass ratios may represent the most highly evapoconcentrated seawater which interacted with late-stage evaporite minerals upon nearing the (current-day) southeastern margin of the Elk Point Basin. The conceptual model shown in [Figure 5](#) requires conditions of progressive evapoconcentration of water moving within the Elk Point Basin at a rate sufficient to maintain salt concentrations of less than potash-mineral saturation near the basin's southeastern margin. Such conditions could be met by an influx of open-marine water during a period of sea-level rise offset by evaporation of seawater combined with seepage of the resulting brine into the underlying carbonates of the Winnipegosis/Keg River Formation. Higher water levels within the Elk Point Basin, in response to rising sea level, would act to enhance the migration of brine into the Winnipegosis / Keg River Formation.

Li-enrichment of central-regime brines may reflect dissolution of Li-enriched late-stage evaporite minerals. Li-enrichment of western-regime brines likely reflects the contribution of Li-enriched hydrothermal fluids (occurring later than the processes depicted in [Figure 5](#)). The general trends showing the potential effects of evaporation, hydrothermal activity and dilution with meteoric water on the O and H isotopic compositions of central- and western-regime brines are illustrated in [Figure 6](#). The timing of hydrothermal activity potentially related to Li-enrichment of western-regime brines is uncertain. If hydrothermal activity concurred with a major tectonic event, emplacement of Li-enriched fluids could have taken place in association with the Laramide Orogeny as late as Cretaceous time.

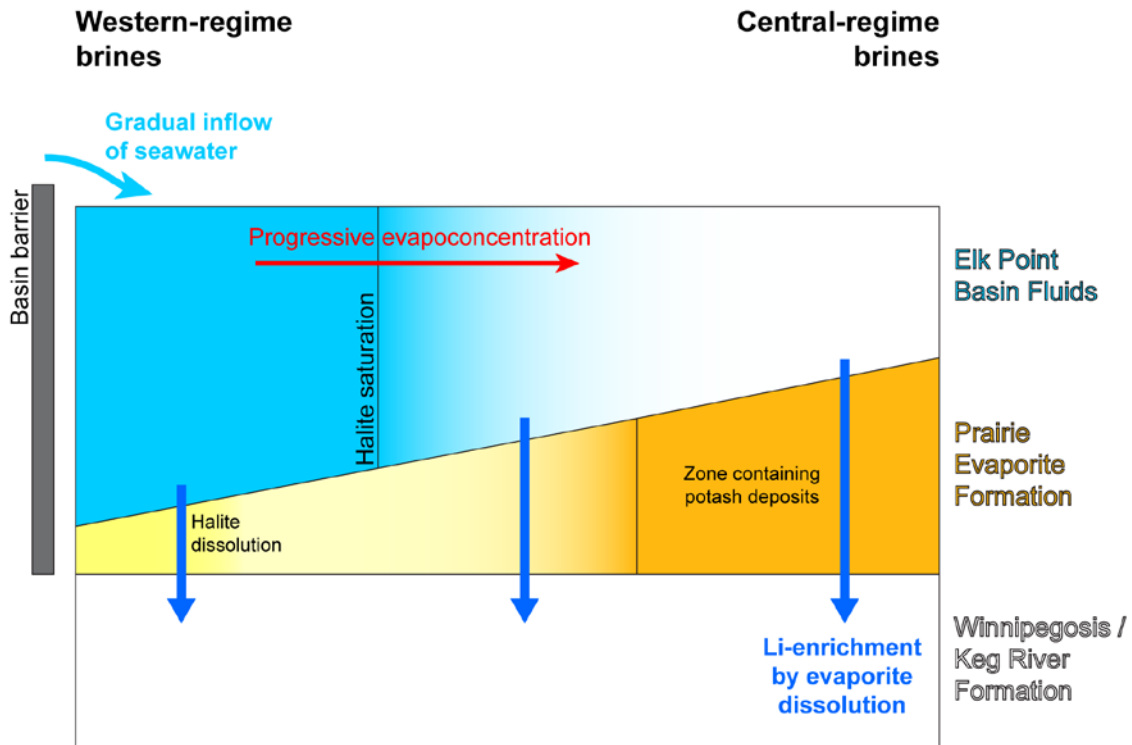


Figure 5. Conceptual model of brine formation within the Devonian Elk Point Basin.

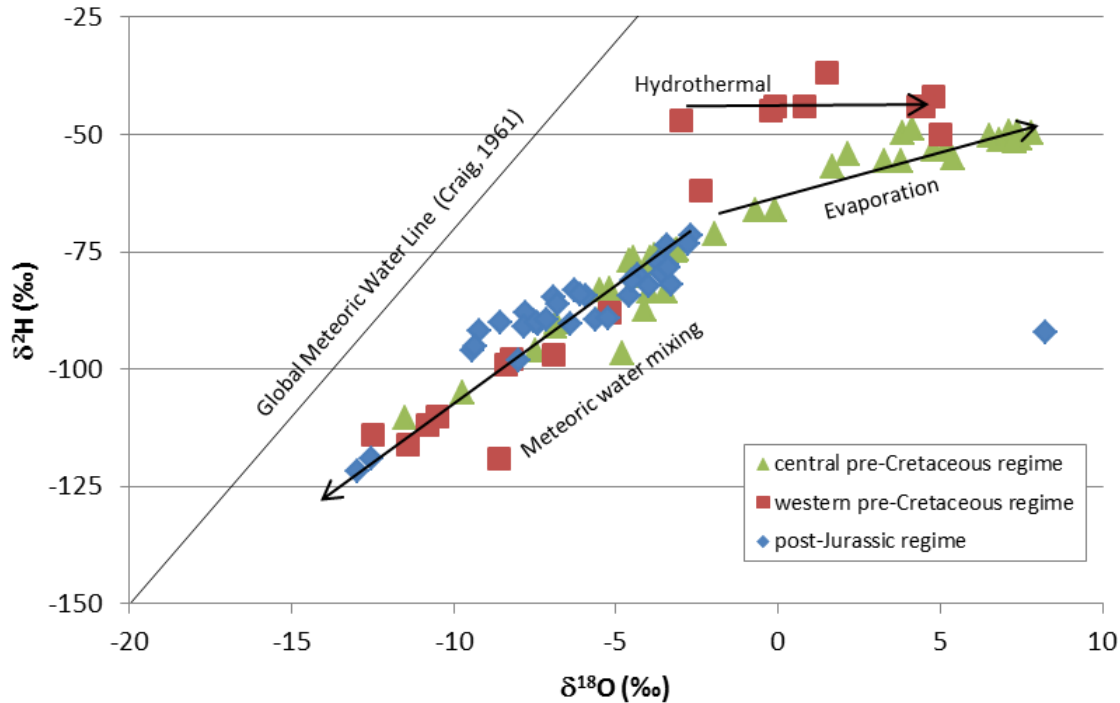


Figure 6. $\delta^{18}\text{O}$ versus $\delta^2\text{H}$ values showing trends in post-Jurassic and pre-Cretaceous regime brines.

5 Summary

Oilfield brines investigated in this study occupy both the pre-Cretaceous and post-Jurassic regional groundwater flow regimes within the Alberta Basin. Pre-Cretaceous regime samples primarily represent Devonian carbonates units while post-Jurassic regime samples primarily represent Cretaceous siliciclastic units. Pre-Cretaceous regime brines lying east (central-regime brines) of the western margin of the Cooking Lake platform show differing properties and have differing evolutionary histories than those lying to the west (western-regime brines) of the platform margin.

Pre-Cretaceous central-regime brines evolved through progressive evapoconcentration of mid-Devonian seawater to, but not past, the point of halite saturation. Progressive evapoconcentration of central-regime brines took place as mid-Devonian seawater moved from the open-marine connection toward the southeastern margin of the Devonian Elk Point Basin. The composition of brines nearing the southeastern margin of the Elk Point Basin was further modified by dissolution of late-stage evaporite (potash) minerals of the Prairie Evaporite Formation. Dense brines generated by evapoconcentration and evaporite mineral dissolution infiltrated into the underlying Winnipegosis / Keg River Formation and were subsequently transported westward by gravitationally-driven flow following regional westward tilting. Regionally-upward groundwater flow associated with Laramide tectonism forced central-regime brines upward into the carbonate complexes of the Nisku and Leduc Formations. Li-enrichment of western-regime brines was caused by dissolution of Li-enriched late-stage evaporite minerals.

Pre-Cretaceous western-regime brines evolved through possible evapoconcentration of mid-Devonian seawater to a point short of halite saturation, followed by dissolution of pre-existing halite deposits. Li-enrichment of western-regime brines likely does not represent evaporative processes or interaction with evaporite minerals but, rather, reflects the contribution of Li-enriched hydrothermal fluids.

6 References

- Bachu, S. (1995): Synthesis and model of formation-water flow, Alberta Basin, Canada; American Association of Petroleum Geologists Bulletin, v. 79, p. 1159–1178.
- Bachu, S. (1999): Flow systems in the Alberta Basin: Patterns, types and driving mechanisms; Bulletin of Canadian Petroleum Geology, v. 47, p. 455–474.
- Billings, G.K., Hitchon, B. and Shaw, D.R. (1969): Geochemistry and origin of formation waters in the Western Canada Sedimentary Basin: 2. Alkali metals; Chemical Geology, v. 4, p. 211–223.
- Burke, W.H., Denison, R.E., Hetherington, E.A., Koepnick, R.B., Nelson, H.F. and Otto, J.B. (1982): Variation of seawater $^{87}\text{Sr}/^{86}\text{Sr}$ throughout Phanerozoic time; Geology, v. 10, p. 516–519.
- Chan, L., Starinsky, A. and Katz, A. (2002): The behavior of lithium and its isotopes in oilfield brines: Evidence from the Heletz-Kokhav field, Israel; Geochimica et Cosmochimica Acta, v. 66, p. 615–623.
- Clayton, R.N., Friedman, I., Graf, D.L., Mavenda, T.K., Meents, W.F. and Shimp, N.F. (1966): The origin of saline formation waters: 1. Isotopic composition; Journal of Geophysical Research, v. 71, p. 3869–3882.
- Collins, A.G. (1976): Lithium abundance in oilfield waters, in Lithium resources and requirements by the year 2000 in Vine, J.D, ed. U.S. Geological Survey Professional Paper 1005, p. 116–123.
- Connolly, C.A., Walter, L.M., Baadsgaard, H. and Longstaffe, F.J. (1990): Origin and evolution of formation waters, Alberta Basin, Western Canada sedimentary basin. I. Chemistry; Applied Geochemistry, v. 5, p. 375–395.
- Connolly, C.A., Walter, L.M., Baadsgaard, H. and Longstaffe, F.J. (1990): Origin and evolution of formation waters, Alberta Basin, Western Canada sedimentary basin. II. Isotope systematics and water mixing; Applied Geochemistry, v. 5, p. 397–411.
- Craig, H. (1961): Isotopic variations in meteoric waters; Science, v. 133, p. 1702–1703.
- Drever, J.I. (1982): The geochemistry of natural waters; Prentice-Hall, Englewood Cliffs, New Jersey, USA, 388 p.
- Eccles D.R. and Berhane, H. (2011): Geological introduction to lithium-rich water with emphasis on the Fox Creek area of west-central Alberta (NTS 83F and 83K); Energy Resources Conservation Board, ERCB/AGS Open File Report 2011-10, 22 p. URL <https://www.ags.aer.ca/publications/OFR_2011_10.html> [February, 2019].
- Garrett, D.E. (2004): Handbook of lithium and natural calcium chloride; Elsevier Academic Press, Oxford, United Kingdom, 488 p.
- Grobe, M. (2000): Distribution and thickness of salt within the Devonian Elk Point Group, Western Canada Sedimentary Basin; Alberta Energy and Utilities Board, EUB/AGS Earth Sciences Report 2000-02, 35 p., URL <https://ags.aer.ca/publications/ESR_2000_02.html> [February, 2019]
- Gupta, I., Wilson, A.M. and Rostron, B.J. (2012): Cl/Br compositions as indicators of the origin of brines: Hydrogeologic simulations of the Alberta Basin, Canada; Geological Society of America Bulletin, v. 124, p. 200–212.
- Hamilton, W.N. (1971): Salt in east-central Alberta; Research Council of Alberta, RCA/AGS Bulletin 29, 65 p. URL <https://ags.aer.ca/publications/BUL_029.html> [February, 2019]
- Hitchon, B. (1969): Fluid flow in the Western Canada Sedimentary Basin, 2: Effect of geology; Water Resources Research, v. 5, p. 460–469.

- Hitchon, B. (1984): Geothermal gradients, hydrodynamics, and hydrocarbon occurrence, Alberta, Canada; Bulletin of the American Association of Petroleum Geologists, v. 68, p. 713–743.
- Hitchon, B., Billings, G.K. and Klovan, J.E. (1971): Geochemistry and origin of formation waters in the Western Canada Sedimentary Basin: III. Factors controlling chemical composition; Geochimica et Cosmochimica Acta, v. 35, p. 567–598.
- Hitchon, B. and Friedman, I. (1969): Geochemistry and origin of formation waters in the Western Canada Sedimentary Basin. I. Stable isotopes of hydrogen and oxygen; Geochimica et Cosmochimica Acta, v. 33, p. 1321–1349.
- Hitchon, B., Underschultz, J.R. and Bachu, S. (1993): Industrial mineral potential of Alberta formation waters; Alberta Research Council, ARC/AGS Open File Report 1993-15, 92 p. URL <https://ags.aer.ca/publications/OFR_1993_15.html> [February, 2019]
- Holser, W.T. (1979a): Mineralogy of evaporites; Reviews in Mineralogy and Geochemistry, v. 6, Chapter 8, p. 210–294.
- Holser, W.T., 1979b, Trace elements and isotopes in evaporites: Reviews in Mineralogy and Geochemistry, v. 6, Chapter 9, p. 295–346.
- Holter, M.E. (1969): The middle Devonian Prairie Evaporite of Saskatchewan; Saskatchewan Department of Mineral Resources Report no. 123, 133 p.
- Horita, J., Weinberg, A., Das, N. and Holland, H.D. (1996): Brine inclusions in halite and the origin of the middle Devonian Prairie Evaporites of western Canada; Journal of Sedimentary Research, v. 66, p. 956–964.
- Huff, G.F. (2016): Evolution of Li-enriched oilfield brines in Devonian carbonates of the south-central Alberta Basin, Canada; Bulletin of Canadian Petroleum Geology, v. 64, p. 438–448.
- Huff, G.F., Bechtel, D.J., Stewart, S.A., Brock, E. and Heikkinen, C. (2012): Water geochemical data, Saline Aquifer Project, 2011 (tabular data, tab delimited format); Energy Resources Conservation Board, ERCB/AGS Digital Dataset 2012-0001. URL <https://ags.aer.ca/publications/DIG_2012_0001.html> [February, 2019]
- Huff, G.F., Lopez, G.P. and Weiss, J.A. (2019): Water geochemistry of selected formation brines in the Alberta Basin, Canada (tabular data, tab delimited); Alberta Energy Regulator / Alberta Geological Survey, AER/AGS Digital Data Release 2019-0002. URL <https://www.ags.aer.ca/publications/DIG_2019-0002.html> [February, 2019]
- Huff, G.F., Stewart, S.A., Riddell, J.T.F and Chisholm, S. (2011): Water geochemical data, Saline Aquifer Project (tabular data, tab delimited format); Energy Resources Conservation Board, ERCB/AGS Digital Dataset 2011-0007. URL <https://www.ags.aer.ca/publications/DIG_2011_0007.html> [February, 2019]
- Lecuyer, C. and Allemant, P. (1999): Modelling the oxygen isotope evolution of seawater: Implications for the climate interpretation of the $\delta^{18}\text{O}$ of marine sediments; Geochimica et Cosmochimica Acta, v. 63, p. 351–361.
- Lico, M.S., Kharaka, Y.K., Carothers, W.W. and Wright, V.A. (1982): Methods for collection and analysis of geopressed geothermal and oil field waters; U.S. Geological Survey Water Supply Paper 2194, 21 p.
- Machel, H.G., Buschkuehle, B.E. and Michael, K. (2001): Squeegee flow in the Devonian carbonate aquifers in Alberta, Canada; *in* Water-Rock Interaction, v. 1, R. Cidu (ed.), Proceedings of the Tenth International Symposium on Water-Rock-Interaction, WRI-10, Villesimius, Italy, p. 631–634.

- Machel, H.G., Cavell, P.A. and Patey, K.S. (1996): Isotopic evidence for carbonate cementation and recrystallization, and for tectonic expulsion of fluids into the Western Canada Sedimentary Basin; *Geological Society of America Bulletin*, v. 108, p. 1108–1119.
- Maiklem, W.R. (1971): Evaporative drawdown – a mechanism for water-level lowering and diagenesis in the Elk Point Basin; *Bulletin of Canadian Petroleum Geology*, v. 19, p. 478–503.
- McCaffrey, M.A., Lazar, B. and Holland, H.D. (1987): The evaporation path of seawater and the coprecipitation of Br⁻ and K⁺ with halite; *Journal of Sedimentary Petrology*, v. 57, p. 928–937.
- Michael, K. and Bachu, S. (2002): Origin, chemistry and flow of formation waters in the Mississippian-Jurassic sedimentary succession in the west-central part of the Alberta Basin, Canada; *Marine and Petroleum Geology*, v. 19, p. 289–306.
- Michael, K., Machel, H.G. and Bachu, S. (2003): New insights into the origin and migration of brines in deep Devonian aquifers, Alberta, Canada; *Journal of Geochemical Exploration*, v. 80, p. 193–219.
- Pană, D and van der Pluijm, B. (2015); Orogenic pulses in the Alberta Rocky Mountains: radiometric dating of major faults and comparison with the regional tectono-stratigraphic record; *GSA Bulletin*, v. 127, p. 480-502.
- Pemberton, S.G. and James, D.P. (ed.) (1997): Petroleum geology of the Cretaceous Mannville Group, western Canada; *Canadian Society of Petroleum Geologists Memoir 18*, p. 169–190.
- Poulton, T.P., Christopher, J.E., Hayes, B.J.R., Losert, J., Tittmore, J., Gilchrist, R.D., Bezys, R. and McCabe, H.R. (1994): Jurassic and lowermost Cretaceous strata of the Western Canada Sedimentary Basin; *in Geological Atlas of the Western Canada Sedimentary Basin*, G.D. Mossop and I. Shetson (comp.), Canadian Society of Petroleum Geologists and Alberta Research Council, p. 297–316. URL <<https://ags.aer.ca/publications/chapter-18-jurassic-and-lowermost-cretaceous-strata>> [February, 2019].
- Price, R.A. (1994): Cordilleran tectonics and the evolution of the Western Canada Sedimentary Basin; *in Geological Atlas of the Western Canada Sedimentary Basin*, G.D. Mossop, and I. Shetson (comp.), Canadian Society of Petroleum Geologists and Alberta Research Council, p. 13–24. URL <<https://ags.aer.ca/publications/chapter-2-cordilleran-tectonics>> [February, 2019].
- Rostron, B.J. and Tóth, J. (1996): Ascending fluid plumes above Devonian pinnacle reefs: numerical modeling and field examples from west-central Alberta, Canada; *in Hydrocarbon migration and its near-surface expression*, D. Schumacher and M.A. Abrams (ed.), American Association of Petroleum Geologists Memoir 66, p. 185-201.
- Rostron, B.J. and Tóth, J. (1997): Cross-formational fluid flow and the generation of a saline plume of formation waters in the Manville Group, west-central Alberta; *in Petroleum geology of the Cretaceous Mannville Group, western Canada*, S.G. Pemberton and D.P. James (ed.), Canadian Society of Petroleum Geologists Memoir 18, p. 169-190.
- Schwerdtner, W.M. (1964): Genesis of potash rocks in the middle Devonian Prairie Evaporite Formation of Saskatchewan; *Bulletin of the American Association of Petroleum Geologists*, v. 48, p. 1108-1115.
- Selleck, B. and Koff, D. (2008): Stable isotope signature of middle Devonian seawater from Hamilton Group brachiopods, central New York State; *Northeastern Geology and Environmental Sciences*, v. 30, p. 330-343.
- Switzer, S.B., W.G., Holland, B.J.R., Christie, D.S., Graf, G.C., Hedinger, A.S., McAuley, R.J., Wierzbicki, R.A. and Packard, J.J. (1994): Devonian Woodbend-Winterburn strata of the Western Canada Sedimentary Basin; *in Geological atlas of the Western Canada Sedimentary Basin*, G.D. Mossop, and I. Shetson (comp.), Canadian Society of Petroleum Geologists and Alberta Research

- Council, p. URL <<https://ags.aer.ca/publications/chapter-12-devonian-woodbend-winterburn-strata.htm>> [February, 2019].
- Streton, D.H. (1967): The geology of the Prairie Evaporite Formation of the Yorkton area of Saskatchewan; M.S. Thesis, University of Saskatchewan, 81 p.
- Underschultz, J.R., Yuan, L.P., Bachu, S., Cotterill, D.K. and Hitchon, B. (1994): Industrial mineral resources in Alberta formation waters; Alberta Research Council, ARC/AGS Open File Report 1994-13, 77 p. URL <https://ags.aer.ca/publications/OFR_1994_13.html> [February, 2019].
- Van der Plank, A. (1962): Petrology and geochemistry of some diamond drill cores from the Saskatchewan potash deposits; M.S. Thesis, University of Wisconsin, 46 p.
- Vengosh A., Starinsky, A., Kolodny, Y., Chivas, A.R. and Rabb, M. (1992): Boron isotope variations during fractional evaporation of sea water: new constraints on the marine vs. nonmarine debate; *Geology*, V. 20, p. 799-802.
- Wallmann, K. (2001): The geological water cycle and the evolution of marine $\delta^{18}\text{O}$ values: *Geochimica et Cosmochimica Acta*, v. 65, p. 2469-2485.
- Walter, L.M., Steuber, A.M., and Huston, T.J. (1990): Br-Cl-Na systematics in Illinois Basin fluids: constraints on fluid origin and evolution; *Geology*, v. 18, p. 315–318.
- Wardlaw, N.C. (1968): Carnallite-sylvite relationships in the middle Devonian Prairie Evaporite Formation, Saskatchewan; *Geological Society of America Bulletin*, v. 79, p. 1273-1294.
- Weast, R.C. and Astle, M.J., ed. (1978): *CRC Handbook of Chemistry and Physics* (59th edition); CRC Press, Boca Raton, Florida.
- White, D.E. (1965): Saline waters of sedimentary rocks; *in* *Fluids in Subsurface Environments*, A. Young and J.E. Galley (eds.), *American Association of Petroleum Geologists Memoir* 4, p. 342-366.
- Wright, G.N., McMechan, M.E. and Potter, D.E.G. (1994): Structure and architecture of the Western Canada Sedimentary Basin, *in* *Geological Atlas of the Western Canada Sedimentary Basin*, G.D. Mossop, and I. Shetson (comp.), *Canadian Society of Petroleum Geologists and Alberta Research Council*, URL <<https://ags.aer.ca/publications/chapter-3-structure-and-architecture.htm>> [February, 2019].
- Yu, X., Zeng, Y., Mu, P., Tan, Q. and Jiang, D. (2015): Solid-liquid equilibria in the quinary system LiCl-KCl-RbCl-MgCl₂-H₂O at T=323K; *Fluid Phase Equilibria*, v. 387, p. 88-94.

Appendix – Plots of Geochemical Data

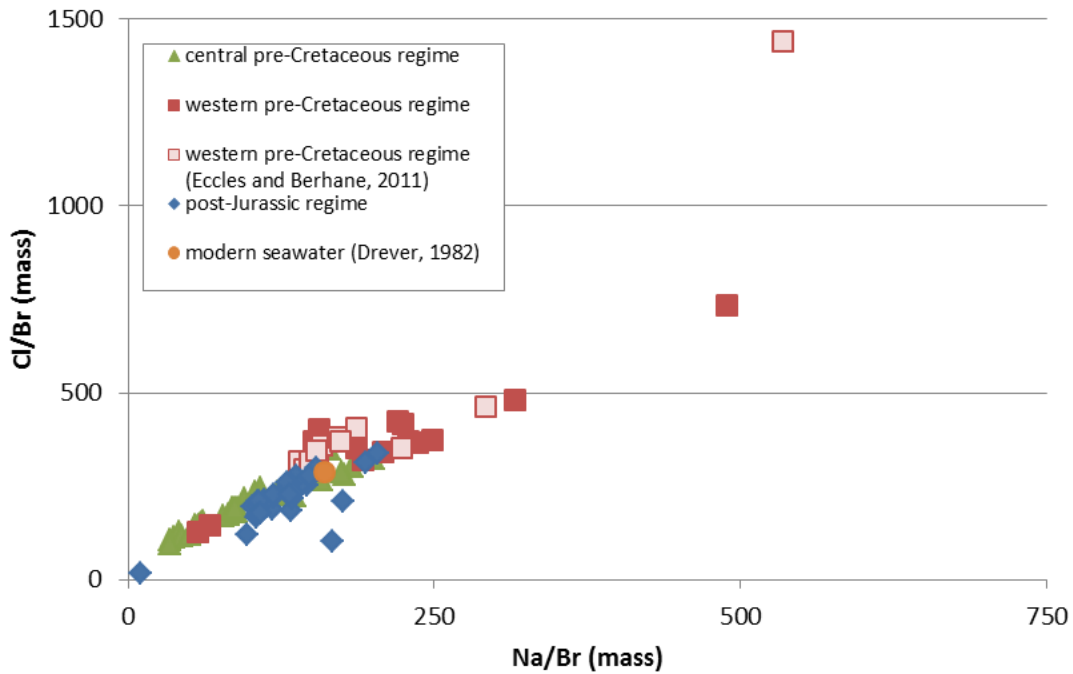


Figure A1-1. Na/Br versus Cl/Br mass ratios in post-Jurassic and pre-Cretaceous regime brines.

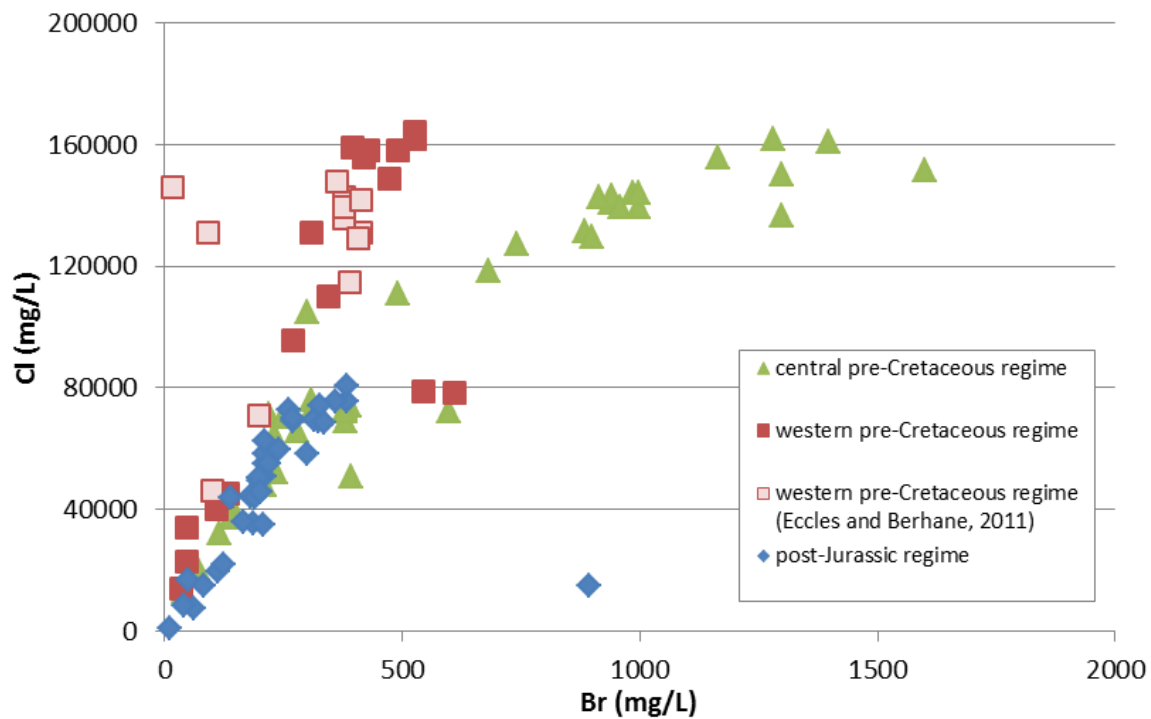


Figure A1-2. Br versus Cl concentrations in post-Jurassic and pre-Cretaceous regime brines.

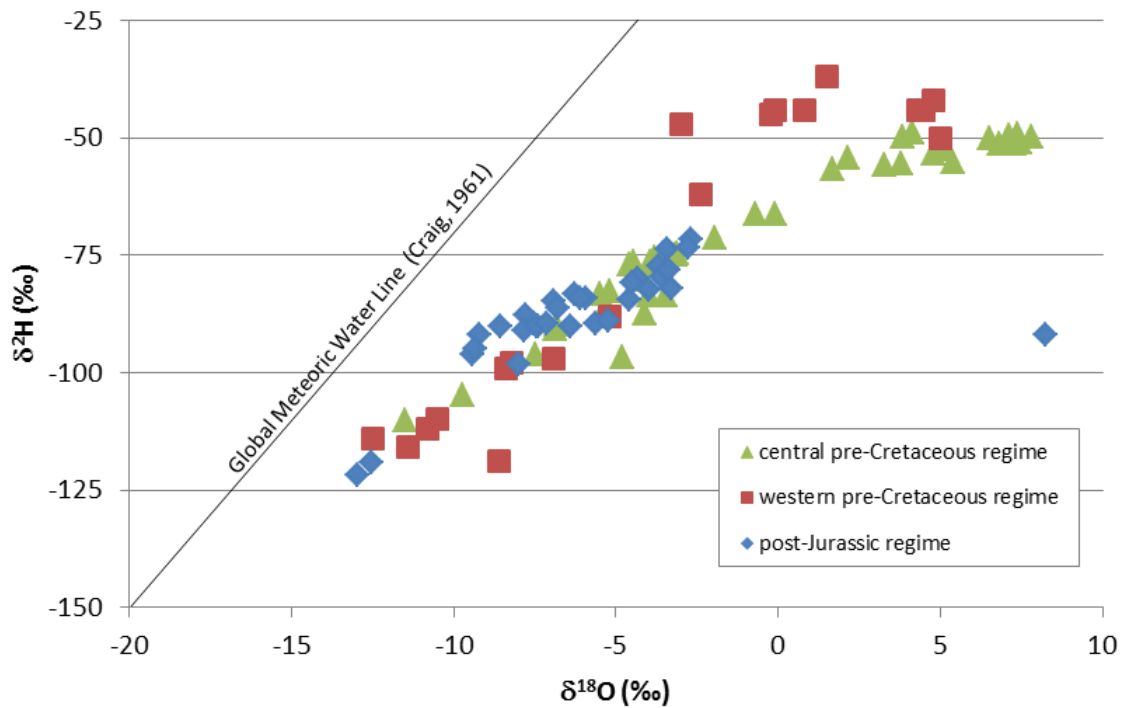


Figure A1-3. $\delta^{18}\text{O}$ versus $\delta^2\text{H}$ values in post-Jurassic and pre-Cretaceous regime brines.

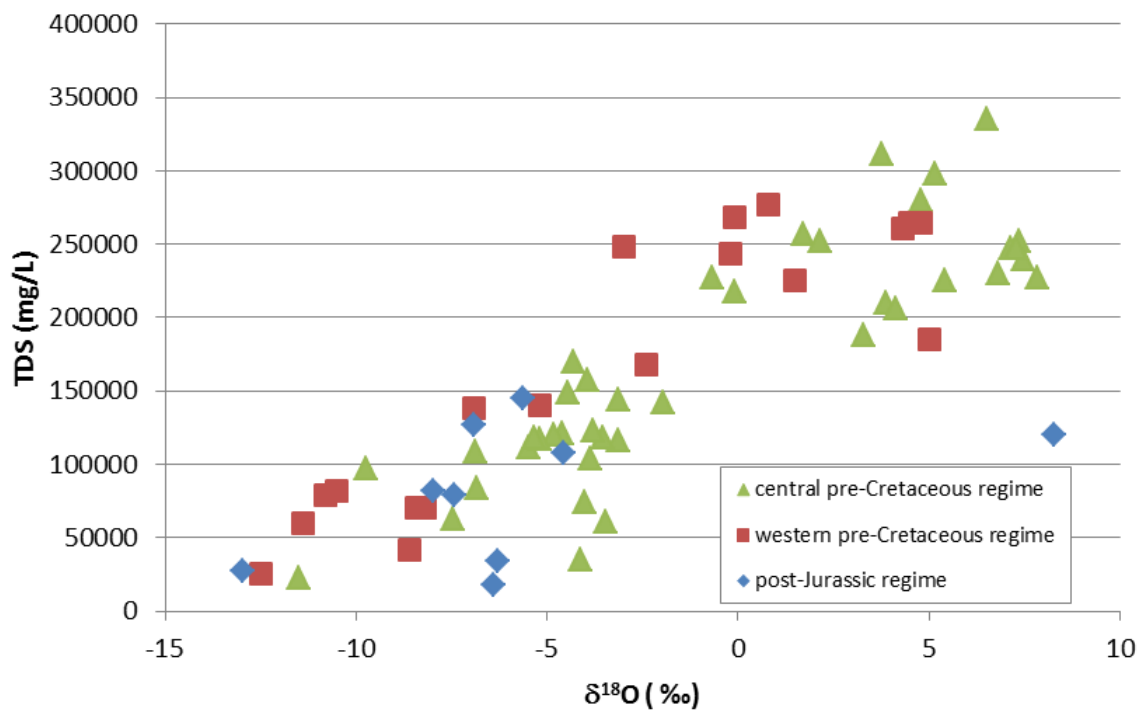


Figure A1-4. Value of $\delta^{18}\text{O}$ versus total dissolved solids concentration in post-Jurassic and pre-Cretaceous regime brines.

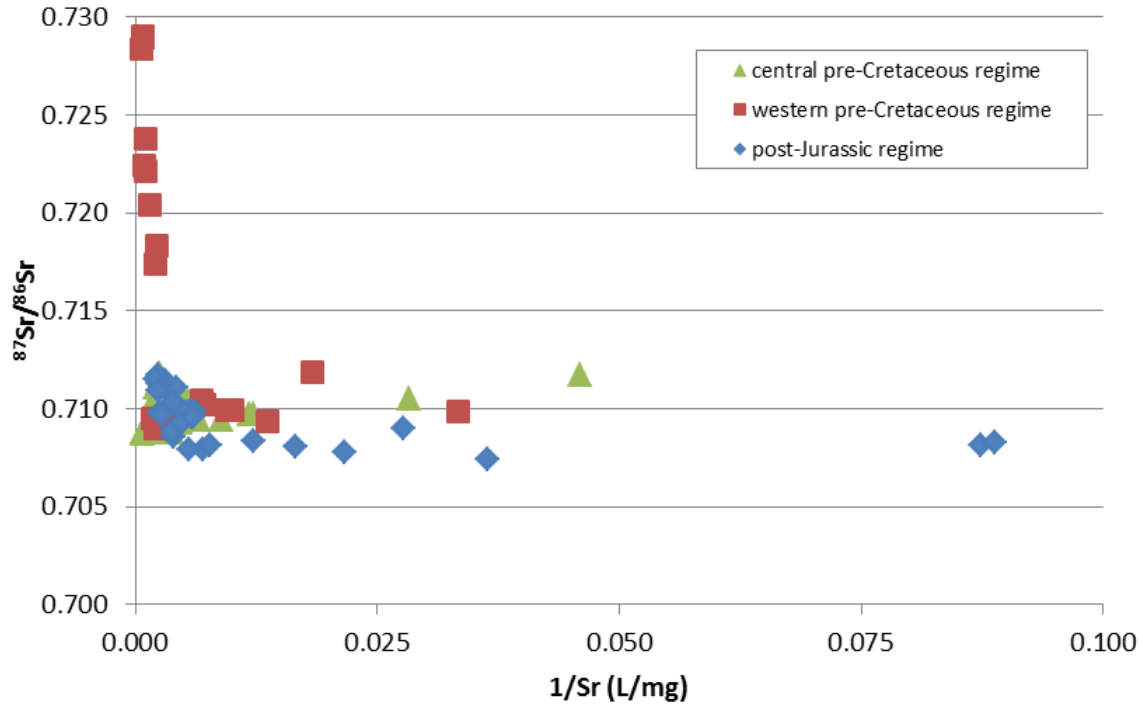


Figure A1-5. Concentration of 1/Sr versus $^{87}\text{Sr}/^{86}\text{Sr}$ value in post-Jurassic and pre-Cretaceous regime brines.

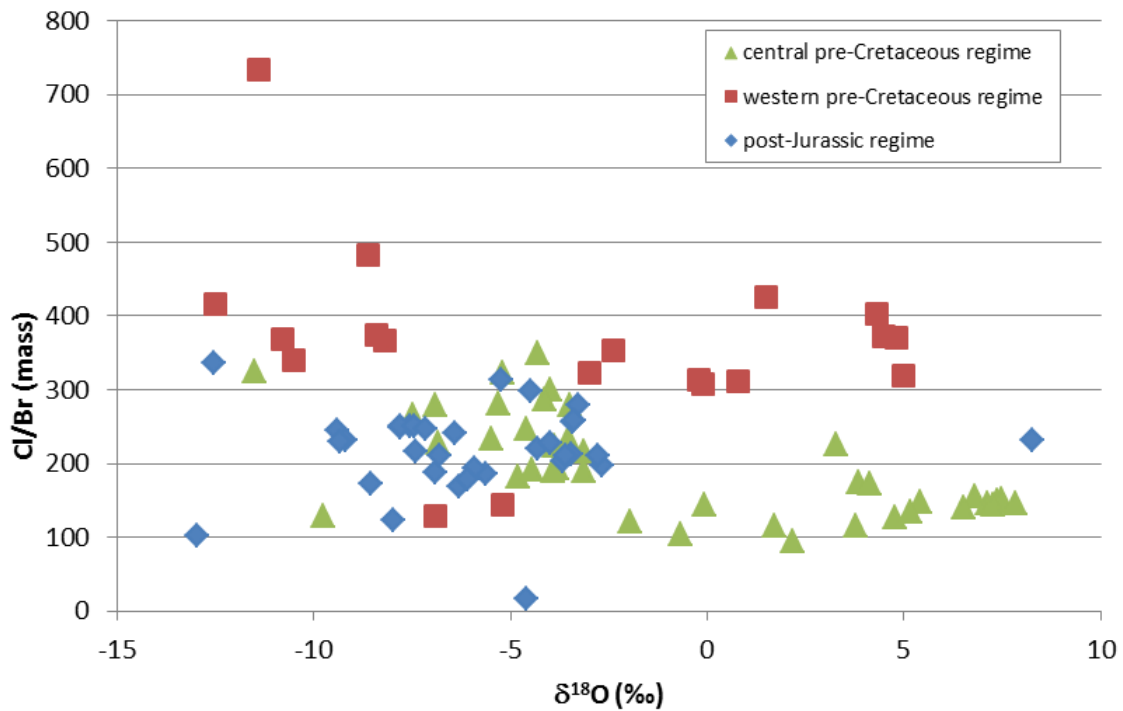


Figure A1-6. Value of $\delta^{18}\text{O}$ versus Cl/Br mass ratio in post-Jurassic and pre-Cretaceous regime brines.

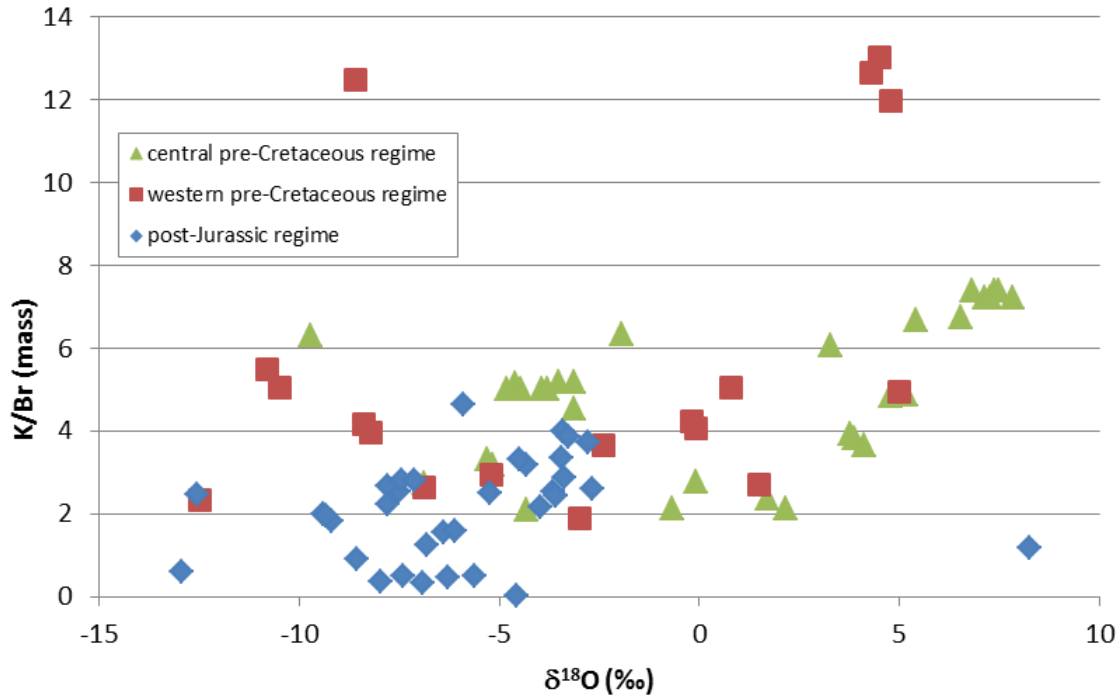


Figure A1-7. Value of $\delta^{18}\text{O}$ versus K/Br mass ratio in post-Jurassic and pre-Cretaceous regime brines.

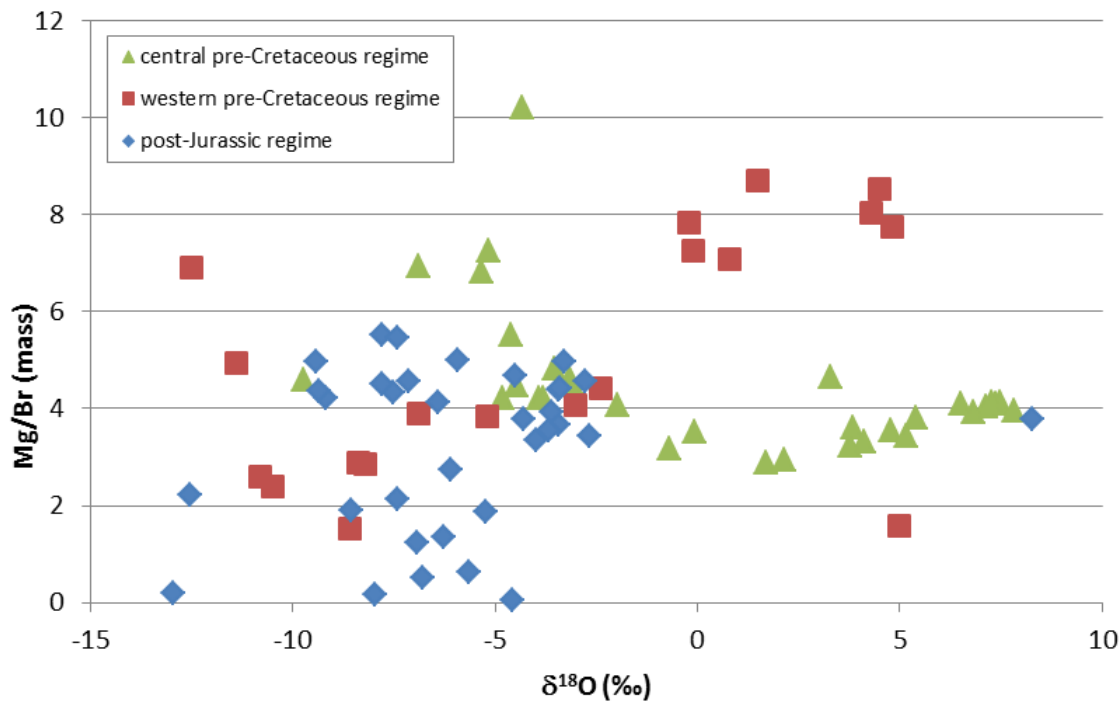


Figure A1-8. Value of $\delta^{18}\text{O}$ versus Mg/Br mass ratio in post-Jurassic and pre-Cretaceous regime brines.

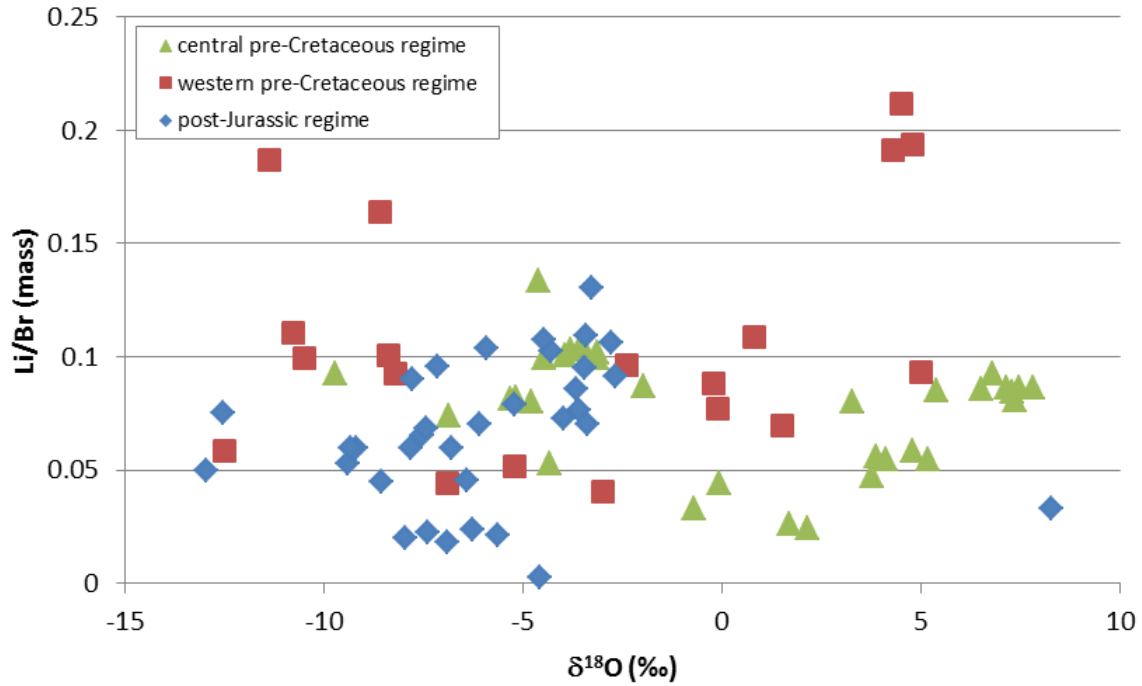


Figure A1-9. Value of $\delta^{18}\text{O}$ versus Li/Br mass ratio in post-Jurassic and pre-Cretaceous regime brines.

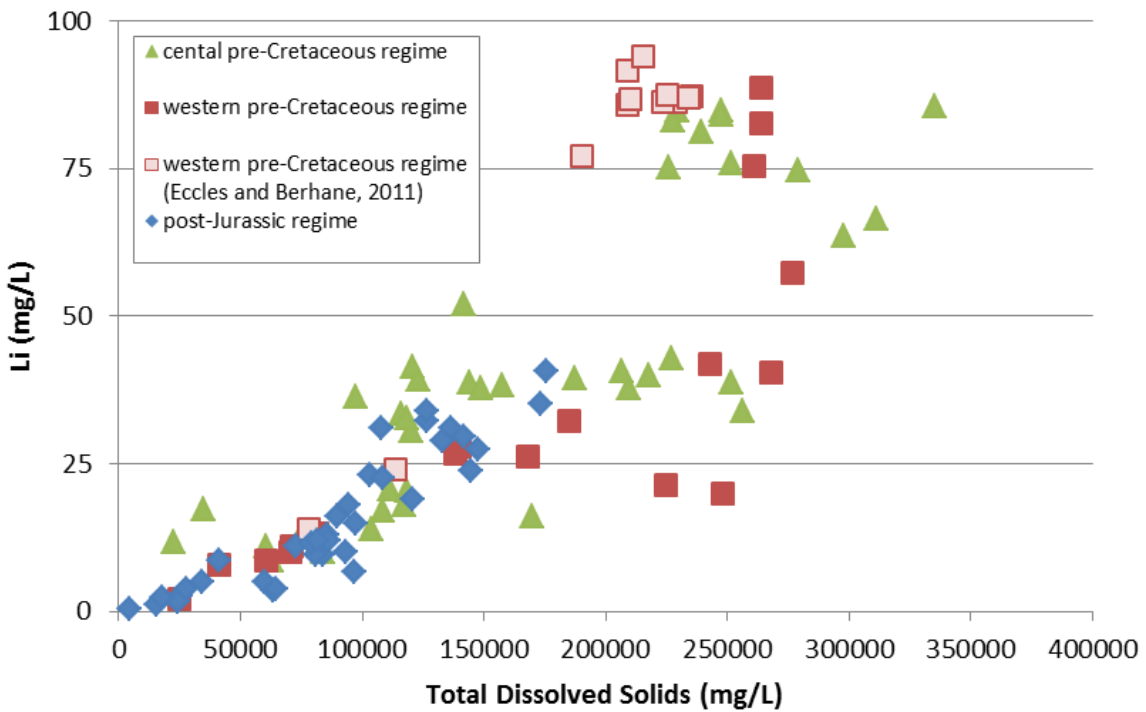


Figure A1-10. Total dissolved solids versus Li concentrations in post-Jurassic and pre-Cretaceous regime brines.

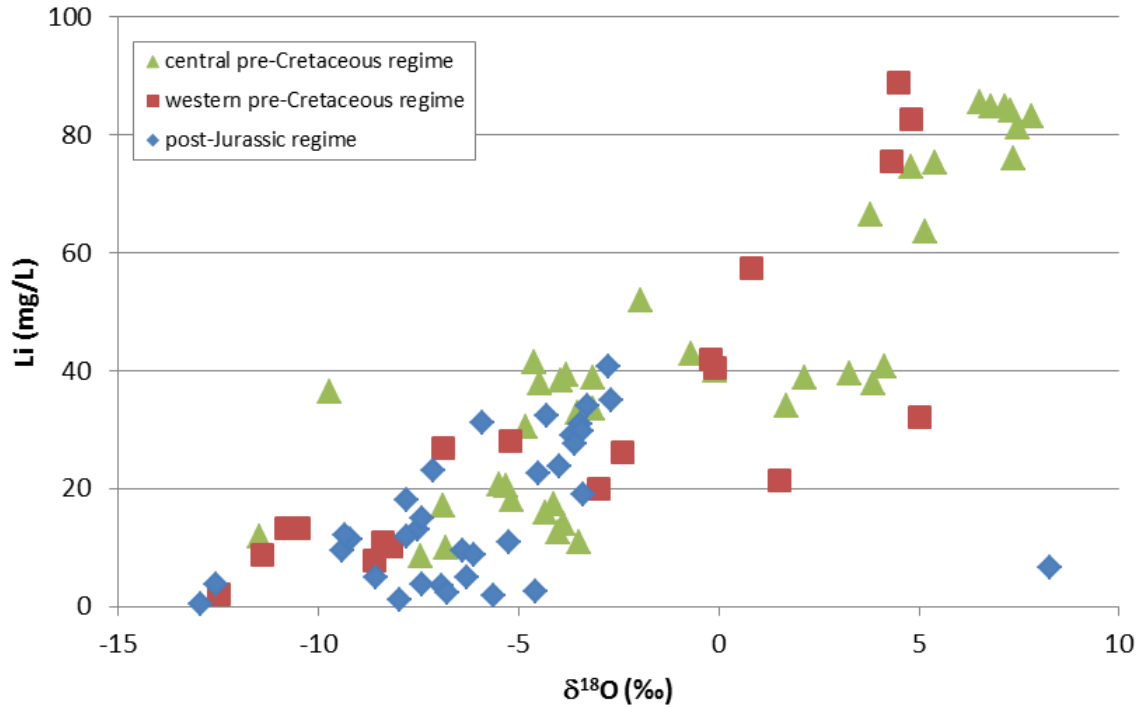


Figure A1-11. Value of $\delta^{18}\text{O}$ versus Li concentration in post-Jurassic and pre-Cretaceous regime brines.

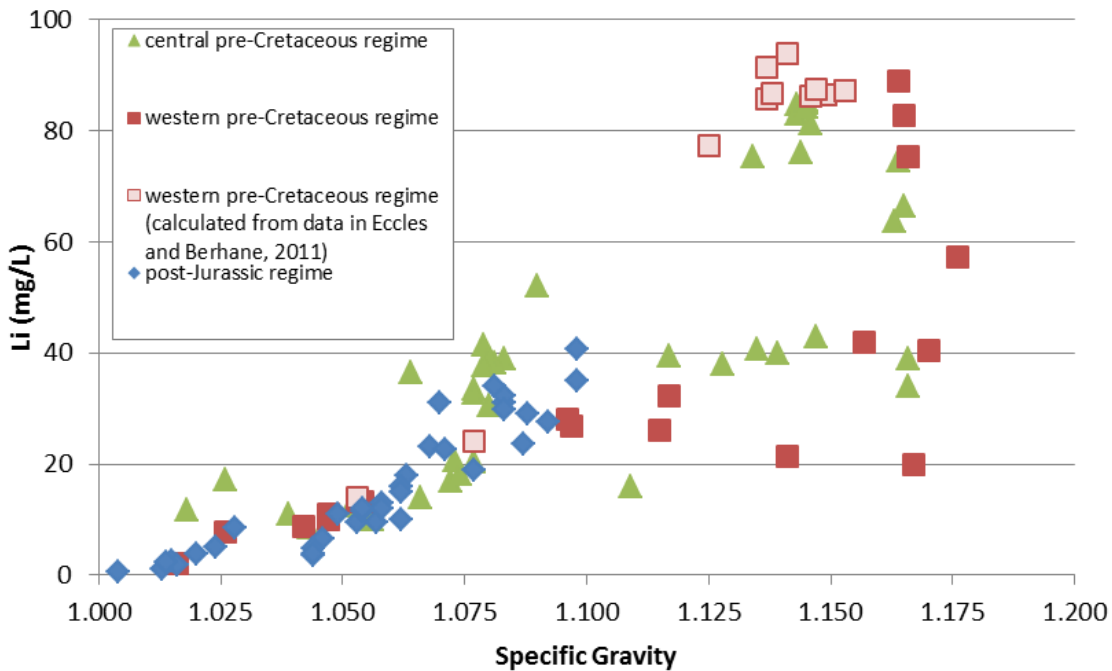


Figure A1-12. Value of specific gravity versus Li concentration in post-Jurassic and pre-Cretaceous regime brines.

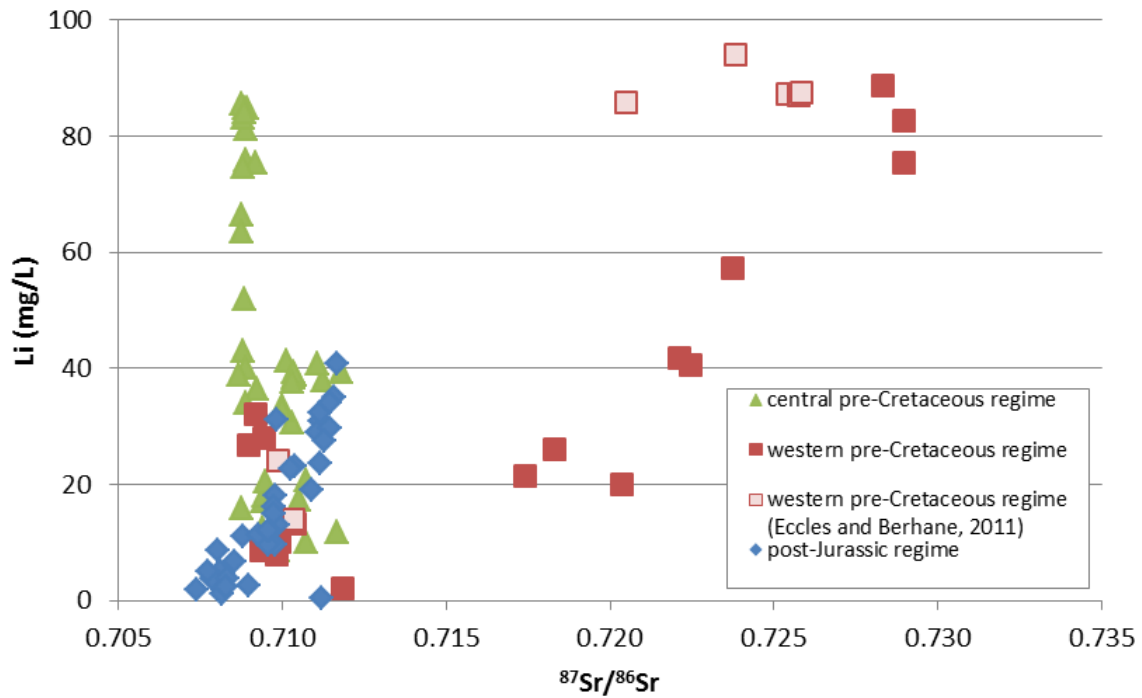


Figure A1-13. Value of $^{87}\text{Sr}/^{86}\text{Sr}$ versus Li concentration in post-Jurassic and pre-Cretaceous regime brines.

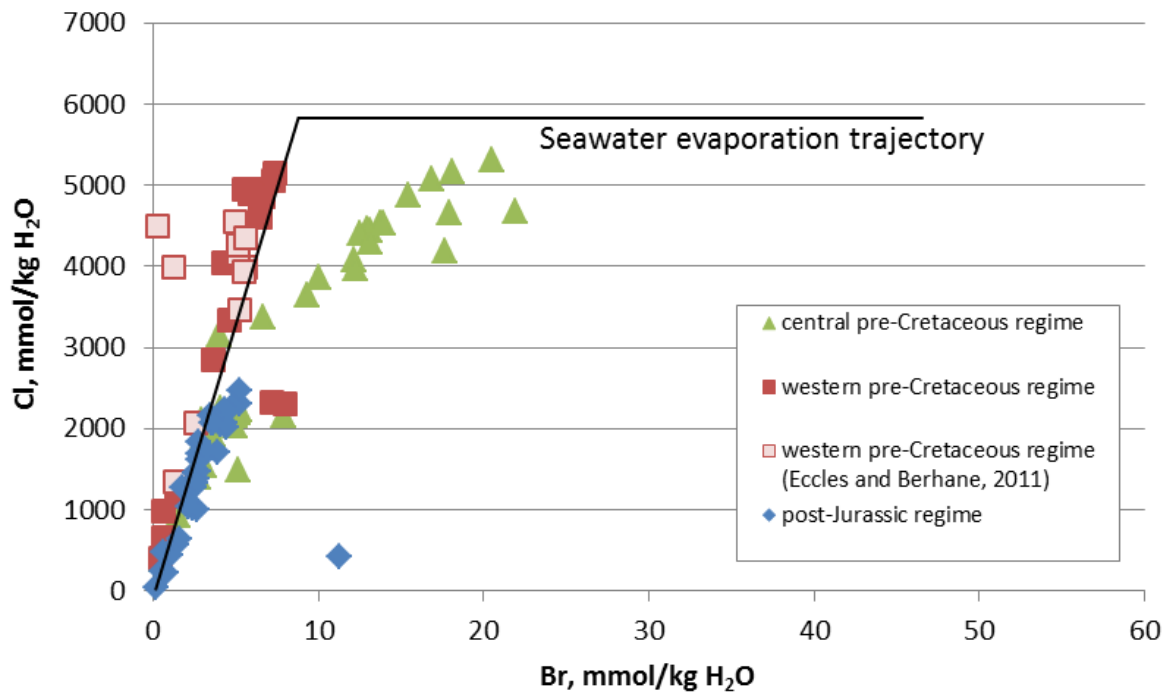


Figure A1-14. Concentrations of Br versus Cl in post-Jurassic and pre-Cretaceous regime brines showing seawater evaporation trajectory derived from McCaffrey et al. (1987).

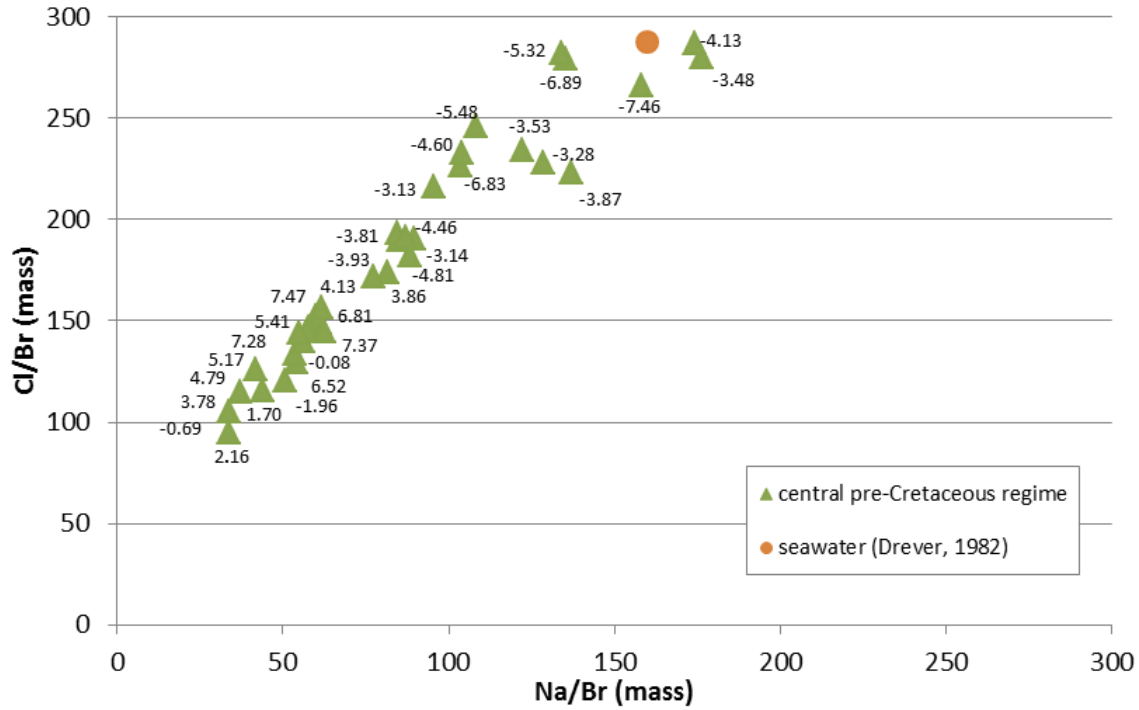


Figure A1-15. Na/Br versus Cl/Br mass ratio showing $\delta^{18}\text{O}$ values in central pre-Cretaceous regime brines.

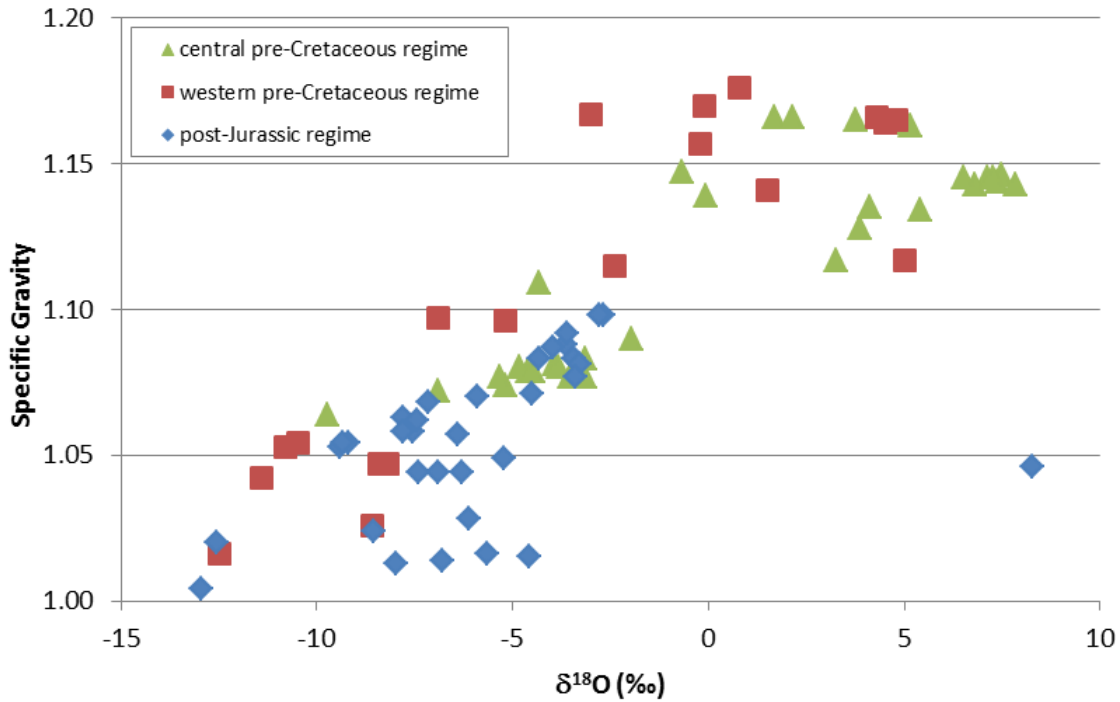


Figure A1-16. Value of $\delta^{18}\text{O}$ versus specific gravity in post-Jurassic and pre-Cretaceous regime brines.

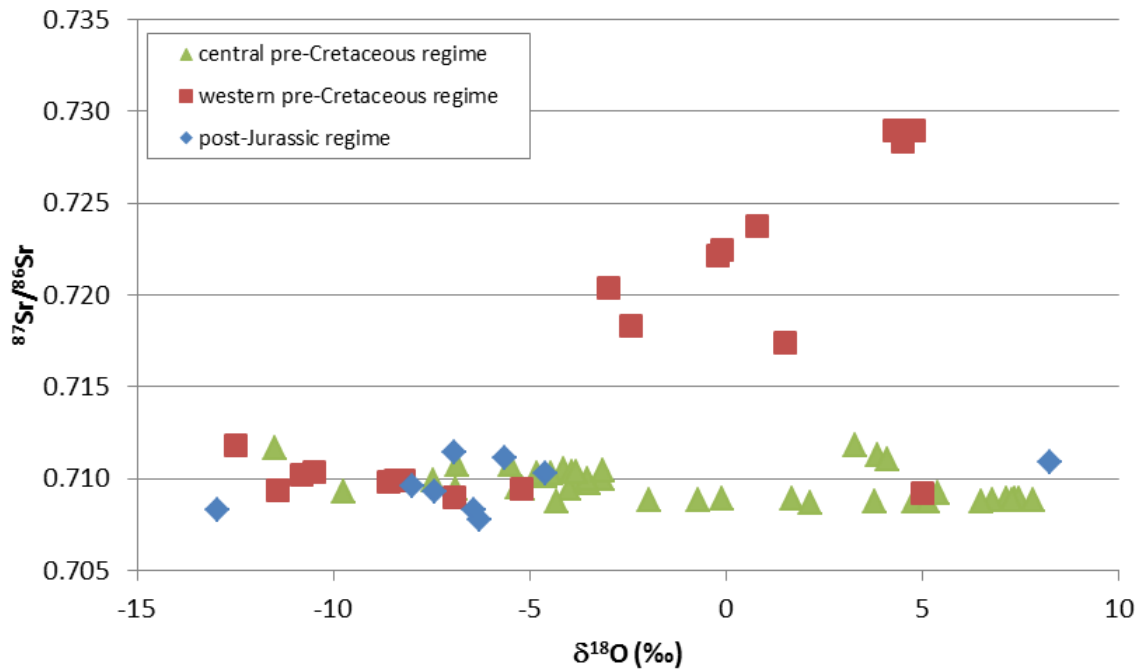


Figure A1-17. Value of $\delta^{18}\text{O}$ versus $^{87}\text{Sr}/^{86}\text{Sr}$ ratio in post-Jurassic and pre-Cretaceous regime brines.

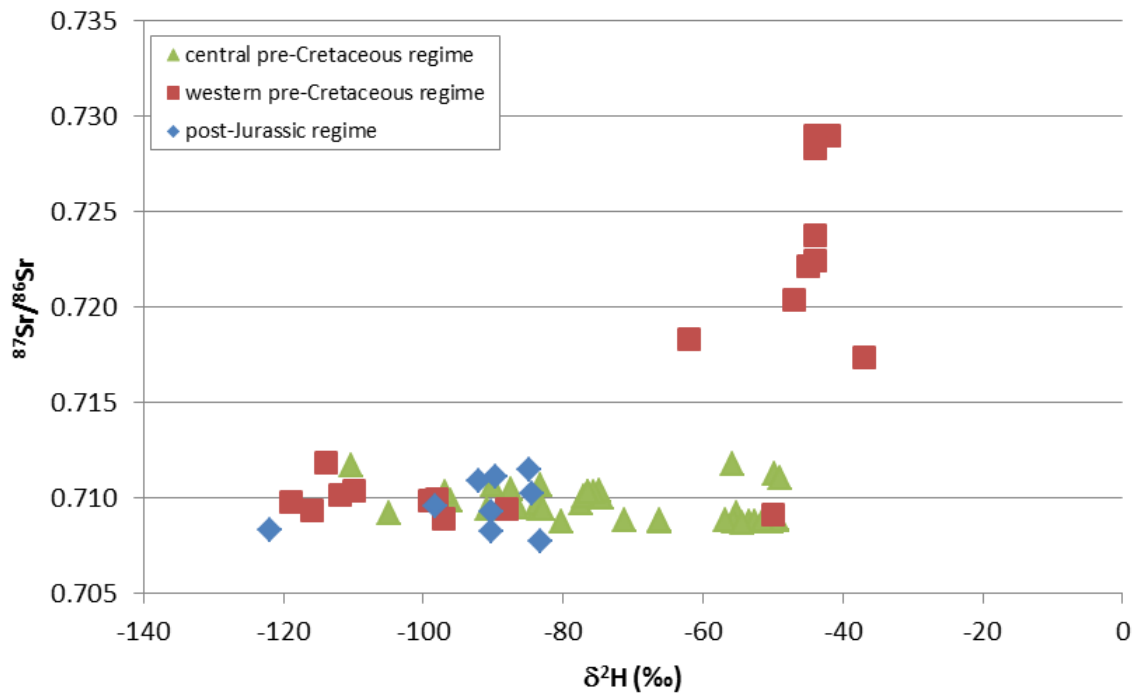


Figure A1-18. Value of $\delta^2\text{H}$ versus $^{87}\text{Sr}/^{86}\text{Sr}$ ratio in post-Jurassic and pre-Cretaceous regime brines.

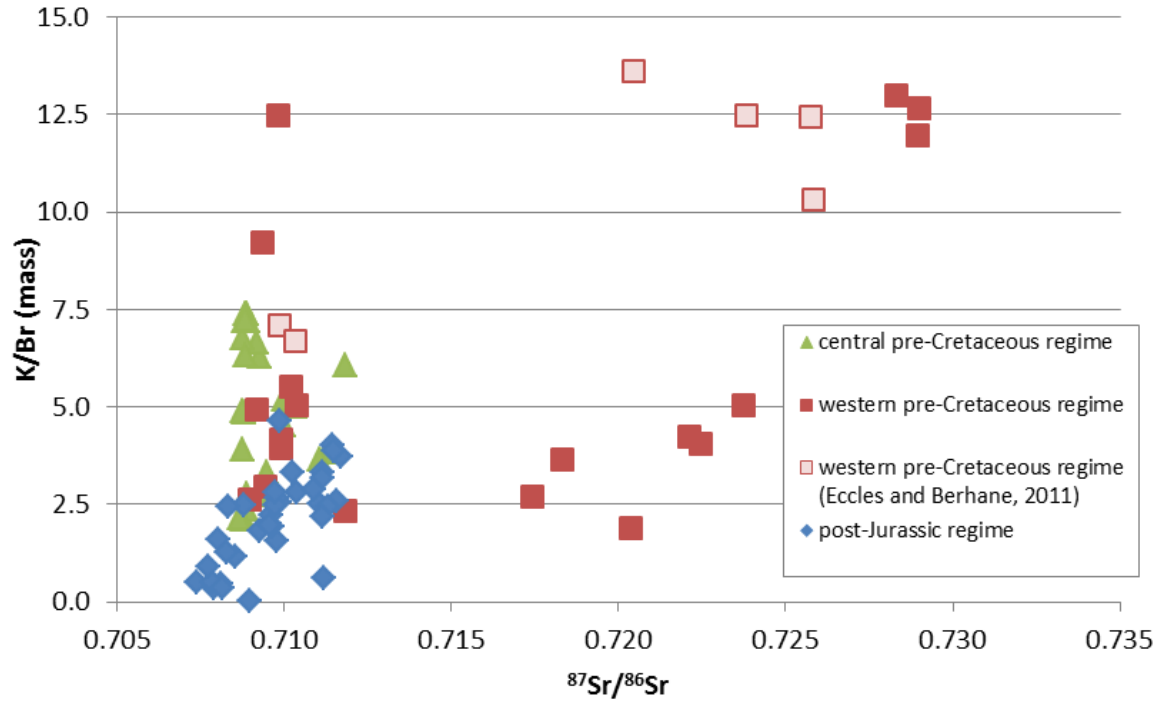


Figure A1-19. Value of $^{87}\text{Sr}/^{86}\text{Sr}$ versus K/Br mass ratio in post-Jurassic and pre-Cretaceous regime brines.

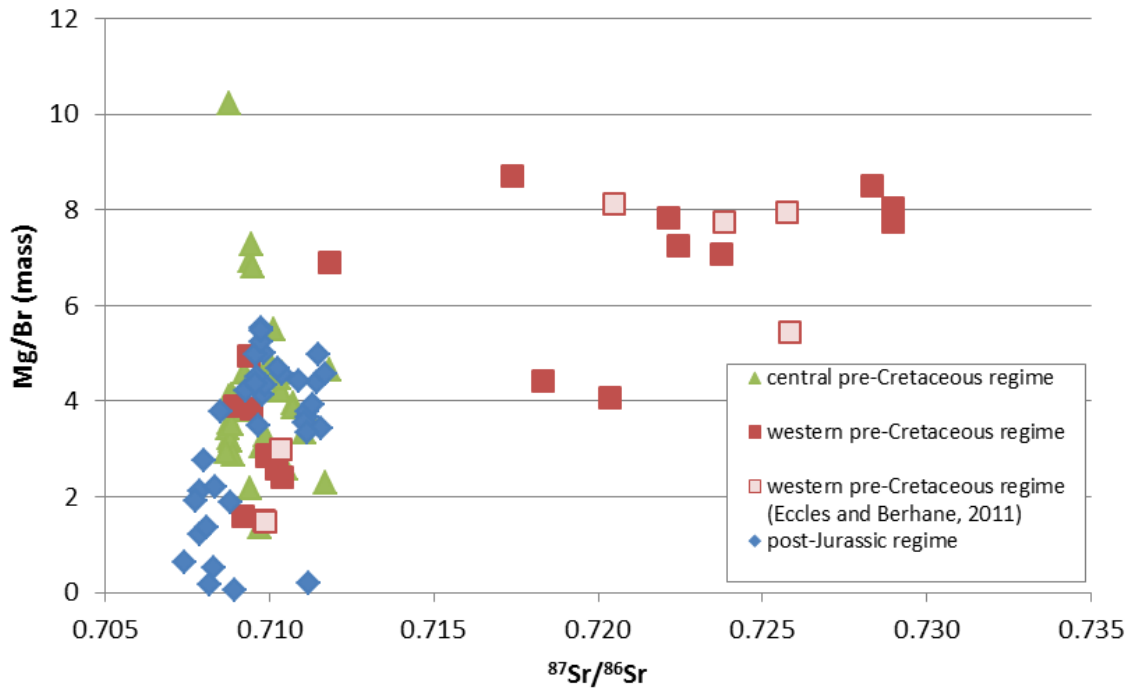


Figure A1-20. Value of $^{87}\text{Sr}/^{86}\text{Sr}$ versus Mg/Br mass ratio in post-Jurassic and pre-Cretaceous regime brines.

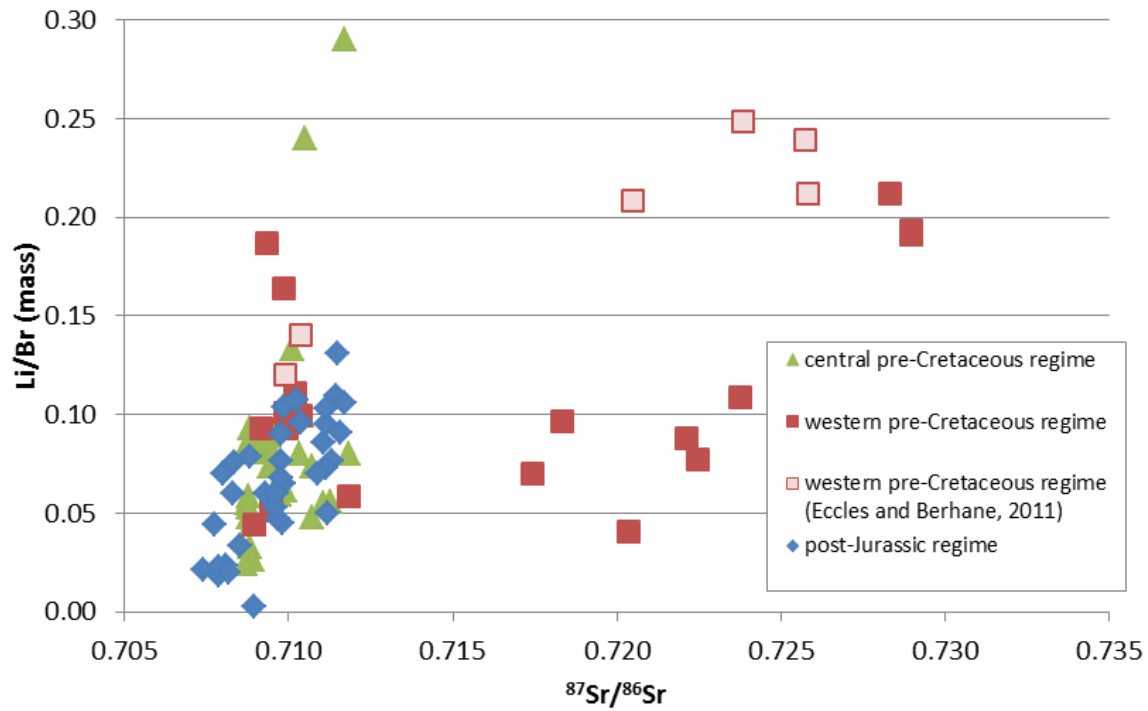


Figure A1-21. Value of $^{87}\text{Sr}/^{86}\text{Sr}$ versus Li/Br mass ratio in post-Jurassic and pre-Cretaceous regime brines.